Journal of Pathology website (*http://www.amjpathol.org*). The tissues were fixed with 4% paraformaldehyde (PFA) or 10% neutral formalin and embedded in paraffin. For the controls, tissue sections were prepared from the autopsied brains of six non-MS neurological and psychiatric disease cases that include a 47-year-old man with acute cerebral infarction who died of sepsis (no. 719), an 84-year-old man with acute cerebral infarction who died of disseminated intravascular coagulation (no. 786), a 62-year-old man with old cerebral infarction who died of pancreatic cancer (no. 789), a 56-year-old man with old cerebral infarction who died of myocardial infarction (no. 807), a 36-year-old woman with schizophrenia who died of lung tuberculosis (no. 523), and a 61-year-old man with schizophrenia who died of asphyxia (no. 826). In addition, they were prepared from the autopsied brains of six neurologically normal patients that include a 79-year-old woman who died of hepatic cancer (no. G6), a 75-year-old woman who died of breast cancer (no. G7), a 60-year-old woman who died of external auditory canal cancer (no. G8), a 74-year-old woman who died of gastric and hepatic cancers (no. G9), an 83-year-old woman who died of gastric cancer and myocardial infarction (no A2623), and a 65-year-old man who died of liver cirrhosis and bronchopneumonia (no. A2647). Autopsies on all patients were performed at the National Center Hospital for Mental, Nervous, and Muscular Disorders, NCNP, Tokyo, Japan. Written informed consent was obtained in all cases.

Immunohistochemistry and Immunocytochemistry

After deparaffination, the tissue sections were heated by microwave at 95°C for 10 minutes in 10 mmol/L citrate sodium buffer (pH 6.0). They were then treated at room temperature for 15 minutes with 3% H_2O_2-containing methanol. For vimentin immunolabeling, the tissue sections were pretreated with 0.125% trypsin solution (Nichirei, Tokyo, Japan) at 37°C for 15 minutes. They were then incubated with 10% normal goat serum containing phosphate-buffered saline (PBS) at room temperature for 15 minutes to block nonspecific staining. The sections were incubated in a moist chamber at 4°C overnight with a panel of 14-3-3 isoform-specific antibodies or with antibodies broadly reactive against all isoforms listed in Table 1. The antibodies were obtained from Immunobiological Laboratory (IBL), Gumma, Japan, and Santa Cruz Biotechnology, Santa Cruz, CA. The specificity of the antibodies from IBL is shown in Supplementary Figure 1 on The American Journal of Pathology website, and additional information on those of Santa Cruz Biotechnology is available on the supplier's website (*www.scbt.com*). After washing with PBS, the tissue sections were labeled at room temperature for 30 minutes with peroxidase-conjugated secondary antibodies (Simple Stain MAX-PO kit, Nichirei) followed by incubation with a colorizing solution containing diaminobenzidine tetrahydrochloride and a counterstain with hematoxylin. To identify cell types expressing the 14-3-3 protein, adjacent sections were stained with the following antibodies: rabbit polyclonal antibody against GFAP (N1506; DAKO, Carpinteria, CA), rabbit polyclonal antibody against vimentin (H-84; Santa Cruz Biotechnology), mouse monoclonal antibody against vimentin (V9; Santa Cruz Biotechnology), rabbit polyclonal antibody against myelin basic protein (N1546; DAKO), mouse monoclonal antibody against CD68 (N1577; DAKO), and mouse monoclonal antibody against 70-kd and 200-kd neurofilament proteins (2F11; Nichirei). For negative controls, sections were incubated with a rabbit-negative control reagent (DAKO) instead of primary antibodies. The optimum concentrations of these antibodies and incubation periods were determined according to the supplier's instruction.

For double-labeling immunocytochemistry, cells on cover glasses were fixed with 4% PFA in 0.1 mol/L phos-

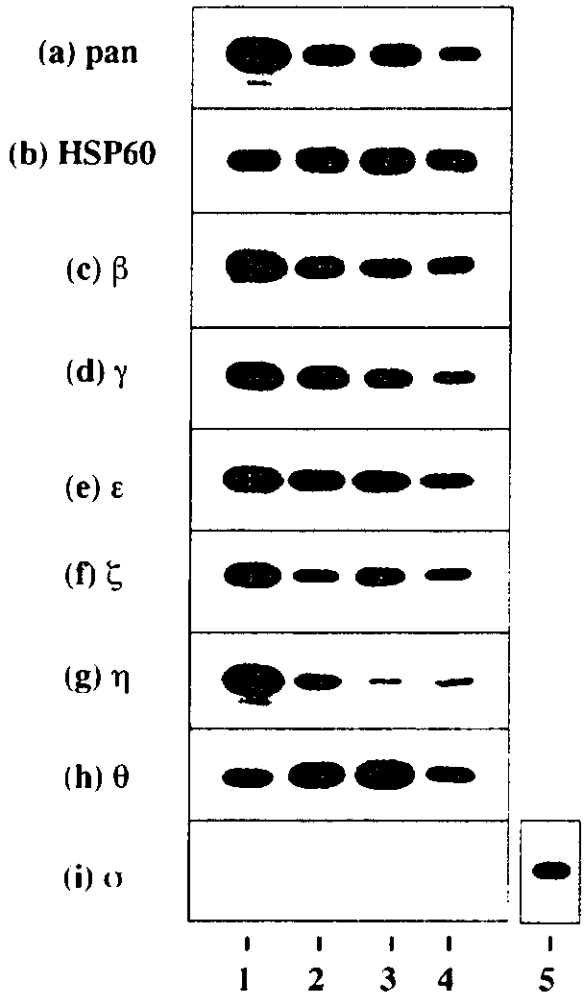

Figure 1. Constitutive expression of 14-3-3 isoforms in cultured human cells. Two μg of total protein extract isolated from brain tissues or cultured cells incubated in 10% FBS containing medium were processed for Western blot analysis using a battery of 14-3-3 isoform specific antibodies or the antibodies broadly reactive against all of the isoforms listed in Table 1, or the antibody against the housekeeping gene product HSP60. **a** to **i** indicate the following antibody specificity: **a**, all isoforms; **b**, HSP60; **c**, β; **d**, γ; **e**, ε; **f**, ζ; **g**, η; **h**, θ; and **i**, σ. **Lanes 1** to **4** represent homogenate of the human cerebrum (**lane 1**), NTera2 derived differentiated neurons (NTera2-N) (**lane 2**), U-373MG astrocytoma cells (**lane 3**), fetal human astrocytes (ASH-77) (**lane 4**), and Hela cervical carcinoma cells (**lane 5**).

phate buffer (pH 7.4) at room temperature for 10 minutes, followed by incubation with PBS containing 0.5% Triton X-100 at room temperature for 20 minutes.[26] The cells were then incubated at room temperature for 30 minutes with a mixture of 14-3-3 isoform-specific antibody and rat monoclonal anti-GFAP antibody (2.2B10) or V9 antibody. Next, they were incubated at room temperature for 30 minutes with a mixture of rhodamine-conjugated anti-rabbit IgG and fluorescein isothiocyanate-conjugated anti-rat or mouse IgG (ICN-Cappel, Aurora, OH). After several washes, cover glasses were mounted on the slides with glycerol-polyvinyl alcohol, and the slides were examined under a Nikon ECLIPSE E800 universal microscope equipped with fluorescein and rhodamine optics. Negative controls were processed following these steps except for exposure to primary antibody.

Cell Culture

Two different sources of cultured human astrocytes were used. One was fetal human astrocytes named AS1477, provided by Drs. K. Watabe and S. U. Kim of the University of British Columbia, Vancouver, BC, Canada. They were maintained in Dulbecco's modified Eagle's medium (DMEM) supplemented with 10% fetal bovine serum (FBS), 100 U/ml penicillin, and 100 μg/ml streptomycin (feeding medium). The other was astrocytes named AS-BW, whose differentiation was induced from neuronal progenitor (NP) cells. NP cells isolated from the brain of a human fetus at 18.5 weeks of gestation were obtained from BioWhittaker (Walkersville, MD). NP cells plated on a polyethyleneimine-coated surface were incubated in DMEM/F-12 medium containing an insulin-transferrin-selenium supplement (Invitrogen, Carlsbad, CA), 20 ng/ml recombinant human epidermal growth factor (Higeta, Tokyo, Japan), 20 ng/ml recombinant human basic fibroblast growth factor (PeproTech EC, London, UK), and 10 ng/ml recombinant human leukemia inhibitory factor (Chemicon, Temecula, CA) (NP medium).[27] For the induction of astrocyte differentiation, NP cells were incubated for several weeks in feeding medium instead of NP medium. This incubation induced vigorous proliferation and differentiation of astrocytes accompanied by a rapid reduction in nonastroglial cell types. Newborn mouse astrocytes were prepared as previously described.[28] In some experiments, cultured human and mouse astrocytes were plated at subconfluent density and incubated for 7 days in serum-free DMEM/F-12 medium supplemented with insulin-transferrin-selenium without inclusion of any other growth factors or in 10% FBS-containing DMEM/F-12 medium supplemented with insulin-transferrin-selenium.

Human cell lines such as U-373MG astrocytoma, NTera2 teratocarcinoma and HeLa cervical carcinoma were obtained from the RIKEN Cell Bank (Tsukuba, Japan) and the American Type Culture Collection (Rockville, MD). For the induction of neuronal differentiation, NTera2 cells maintained in the undifferentiated state (NTera2-U) were incubated for 4 weeks in feeding me-

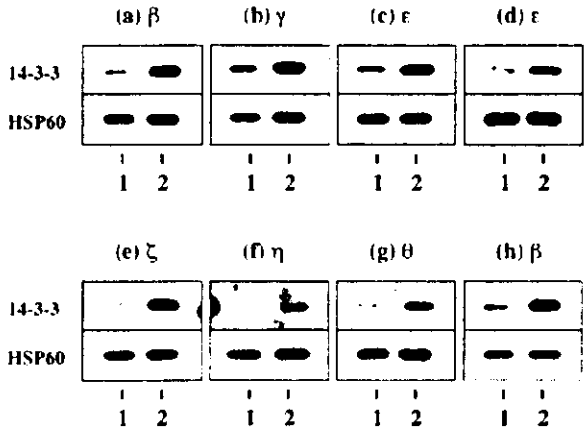

Figure 2. Growth-dependent expression of various 14-3-3 isoforms in cultured human astrocytes. Human and mouse astrocytes were plated at subconfluent density and incubated for 7 days in the serum-free culture medium or in 10% FBS-containing culture medium. Two μg of total protein extract was processed for Western blot analysis using a battery of 14-3-3 isoform-specific antibodies or with the antibodies broadly reactive against all isoforms (**top**). After stripping the antibodies, identical blots were relabeled with the antibody against HSP60 for the standardization of expression levels (**bottom**). **a** to **g** (**top**) indicate the expression of β (**a**), γ (**b**), ε (**c**), ζ (**e**), η (**f**), and θ (**g**) in human astrocytes (AS1477); ε in human astrocytes (AS-BW) (**d**); and β in mouse astrocytes (**h**). **Lanes 1** and **2** represent the cells cultured under the serum-free growth-arrested condition (**lane 1**) or the serum-containing growth-promoting condition (**lane 2**). Additional data are shown in supplementary Figure 2 on the American Journal of Pathology website.

Table 2. Differential Expression of Seven 14-3-3 Isoforms in Glial Cells and Neurons in MS and Control Brains

Brains / 14-3-3 isoforms/cell types	Astrocytes			Microglia/macrophages			Oligodendrocytes			Neurons		
	MS	OND	NNC	MS	OND	NNC	MS	OND	NNC	MS	OND	NNC
β	maj(++)	maj(+)	no( )	maj(++)	maj(++)	no( )	min(+)	no( )	no( )	maj(++)	maj(++)	maj(++)
γ	min(++)	min(+)	no( )	min(++)	min(+)	no( )	no( )	no( )	no( )	maj(++)	maj(++)	maj(++)
ε	maj(++)	maj(++)	min(+)	no( )	no( )	no( )	no( )	no( )	no( )	min(+)	min(+)	min(+)
ζ	maj(++)	maj(++)	no( )	maj(++)	maj(++)	no( )	no( )	no( )	no( )	maj(++)	maj(++)	maj(++)
η	maj(++)	maj(++)	no( )	maj(++)	min(++)	no( )	no( )	no( )	no( )	maj(++)	maj(++)	maj(++)
θ	min(+)	min(+)	no( )	no( )	no( )	no( )	min(++)	min(++)	min(+)	min(+)	min(+)	min(+)
σ	min(++)	min(++)	min(+)	no( )	no( )	no( )	no( )	no( )	no( )	no( )	no( )	no( )

The present study includes four MS cases numbered *#791, 744, 609*, and *544* whose clinical profiles are given in a supplementary table on the AJP website; six non-MS neurological and psychiatric disease cases (OND) composed of *#719* acute cerebral infarction, *#786* acute cerebral infarction, *#789* old cerebral infarction, *#807* old cerebral infarction, *#523* schizophrenia, and *#826* schizophrenia; and six neurologically normal cases (NNC) composed of *#636, #647, #638, #629, #A2623*, and *#A2647*, whose profiles are described in the Materials and Methods section.

The population size of the immunoreactive cells is expressed as maj, major (large) population; min, minor (small) population; and no, almost no population. The intensity of immunoreactivity is graded as ( ) negative, (+) weak, and (++) intense.

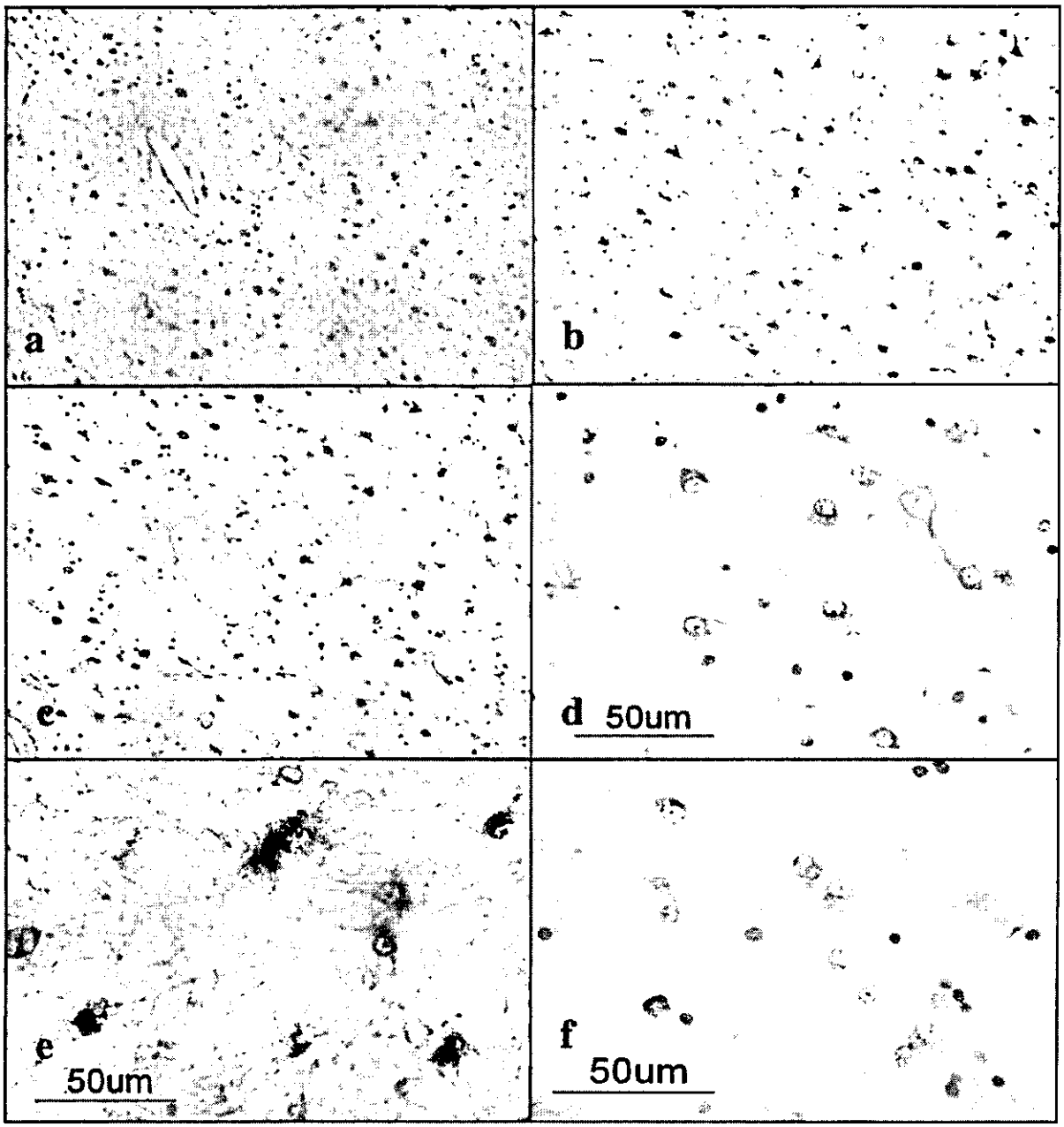

Figure 3. The 14-3-3ε isoform is expressed in reactive astrocytes in chronic demyelinating lesions of MS. MS brain tissues were processed for immunohistochemical analysis using ε isoform specific antibody or the antibody against GFAP or vimentin. **a** to **f** represent the following: **a:** no. 744 MS, chronic active demyelinating lesions in the subcortical white matter of the frontal lobe (H&E). **b:** No. 744 MS, the area corresponding to **a** (GFAP). Many reactive astrocytes are stained. **c:** No. 744 MS, the area corresponding to **a** (ε). Many reactive astrocytes are stained. **d:** No. 744 MS, a higher magnification view of **c** (ε). Reactive astrocytes are stained. **e:** No. 541 MS, chronic inactive demyelinating lesions in the optic nerve (ε). Reactive astrocytes and the glial scar are stained. **f:** No. 744 MS, chronic active demyelinating lesions in the subcortical white matter of the frontal lobe (vimentin). Reactive astrocytes are stained.

dium containing 10^{-5} mol/L *all trans* retinoic acid (Sigma, St. Louis, MO), replated twice and then plated on a surface coated with Matrigel Basement Membrane Matrix (Becton Dickinson, Bedford, MA). They were incubated for another 2 weeks in feeding medium containing a cocktail of mitotic inhibitors, resulting in the enrichment of differentiated neurons (NTera2-N).[36]

Western Blot Analysis

To prepare total protein extract for Western blot analysis, the cells and tissues were homogenized in RIPA lysis buffer composed of 50 mmol/L Tris-HCl (pH 7.5), 150 mmol/L NaCl, 1% Nonidet P-40, 0.5% sodium deoxycholate, 0.1% sodium dodecyl sulfate (SDS), and a cock-

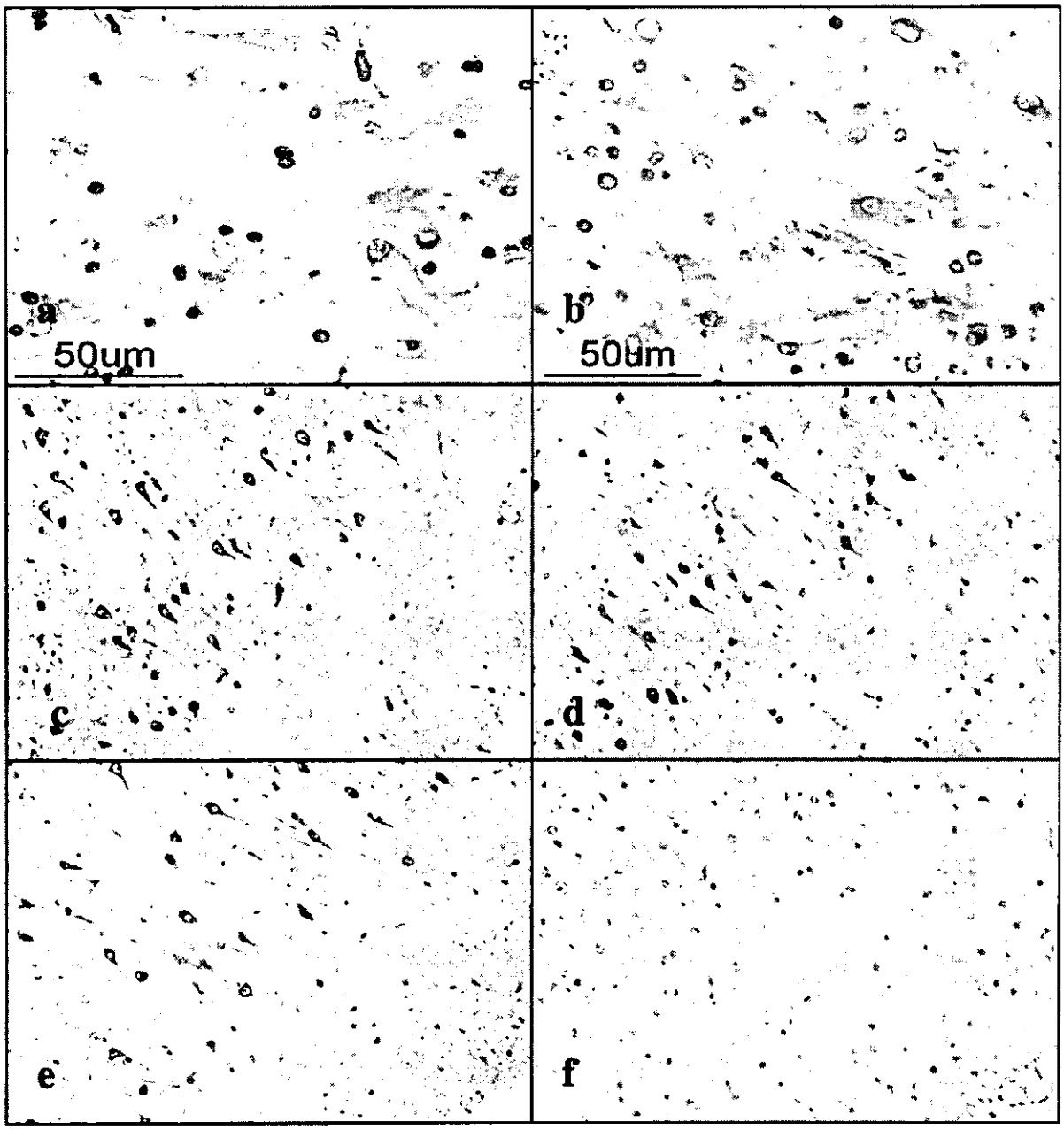

Figure 4. Expression of various 14-3-3 isoforms in reactive astrocytes and cortical neurons in MS brain. MS brain tissues were processed for immunohistochemical analysis using a battery of 14-3-3 isoform specific antibodies. **a** to **f** represent the following: **a:** no. 744 MS, chronic active demyelinating lesions in the subcortical white matter of the frontal lobe (β). Reactive astrocytes are stained. **b:** No. 744 MS, chronic active demyelinating lesions in the subcortical white matter of the frontal lobe (ζ). Reactive astrocytes are stained. **c:** No. 744 MS, the cerebral cortex of the frontal lobe (γ). Cortical neurons are stained. **d:** No. 744 MS, the area corresponding to **c** (γ). Cortical neurons are stained. **e:** No. 744 MS, the area corresponding to **c** (ζ). Cortical neurons are stained. **f:** No. 744 MS, the area corresponding to **c** (ε). Cortical neurons are devoid of staining.

tail of protease inhibitors (Roche Diagnositics, Mannheim, Germany), followed by centrifugation at 12,000 rpm at room temperature for 20 minutes. The supernatant was collected for separation on a 12% SDS-polyacrylamide gel electrophoresis (PAGE) gel and the protein concentration was determined by a Bradford assay kit (Bio-Rad, Hercules, CA). After gel electrophoresis, the protein was transferred onto nitrocellulose membranes and immunolabeled at room temperature overnight with a panel of anti-14-3-3 protein antibodies listed in Table 1. Then, the membranes were incubated at room temperature for 30 minutes with horseradish peroxidase-conjugated anti-rabbit IgG or anti-mouse IgG (Santa Cruz Biotechnology). The specific reaction was visualized with a Western blot detection system using a chemiluminescent substrate (Pierce, Rockford, IL). After the antibodies were stripped

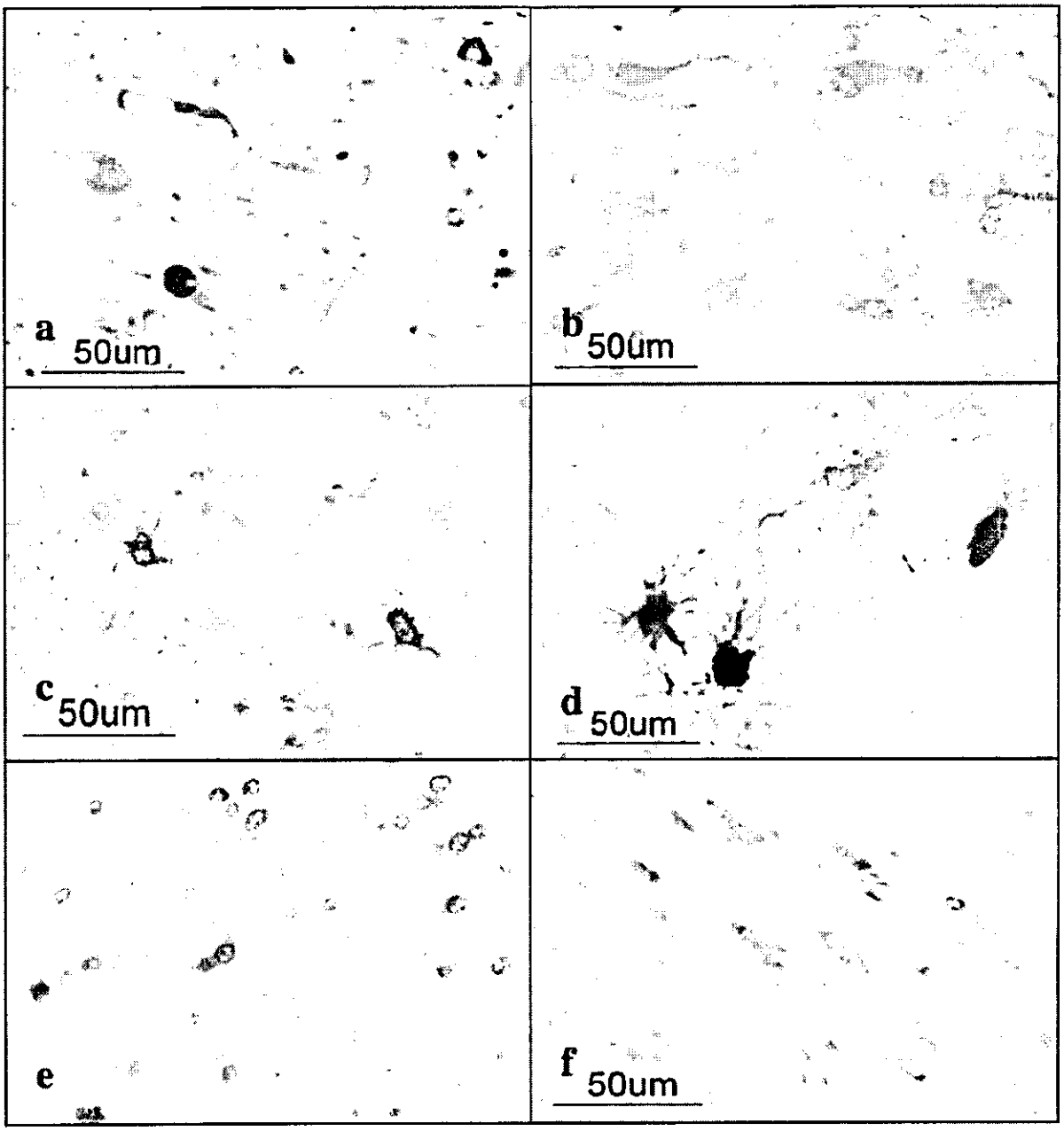

Figure 5. Expression of various 14-3-3 isoforms in reactive astrocytes, surviving oligodendrocytes, and injured axons in chronic demyelinating lesions of MS and in infarcted lesions. The brains of MS and non MS control cases were processed for immunohistochemical analysis using a battery of 14-3-3 isoform specific antibodies. **a** to **f** represent the following: **a:** no. 609 MS, chronic active demyelinating lesions in the medulla oblongata (×). Disrupted axons are stained. **b:** No. 719 acute cerebral infarction, infarcted lesions in the parietal cerebral cortex (×). Reactive astrocytes are stained. **c:** No. 791 MS, chronic inactive lesions in the pons (×). Reactive astrocytes are stained. **d:** No. 719 acute cerebral infarction, infarcted lesions in the parietal cerebral cortex (×). Reactive astrocytes are stained. **e:** No. 609 MS, chronic active demyelinating lesions in the periventricular white matter of the frontal lobe (×). Surviving oligodendrocytes are stained. **f:** No. 744 MS, chronic active demyelinating lesions in the optic nerve (×). Surviving oligodendrocytes are stained.

by incubating the membranes at 50°C for 30 minutes in stripping buffer composed of 62.5 mmol/L Tris-HCl (pH 6.7), 2% SDS, and 100 mmol/L 2-mercaptoethanol, the membranes were processed for relabeling with goat polyclonal antibody against human heat shock protein HSP60 (N-20; Santa Cruz Biotechnology) followed by incubation with horseradish peroxidase-conjugated anti-goat IgG (Santa Cruz Biotechnology). Densitometric analysis was performed using NIH image version 1.61 software to quantify the intensity of the immunoreactive bands.[36]

Immunoprecipitation Experiments

To prepare total protein extract for immunoprecipitation experiments, the cells were homogenized in M-PER lysis buffer (Pierce) with a cocktail of protease inhibitors fol-

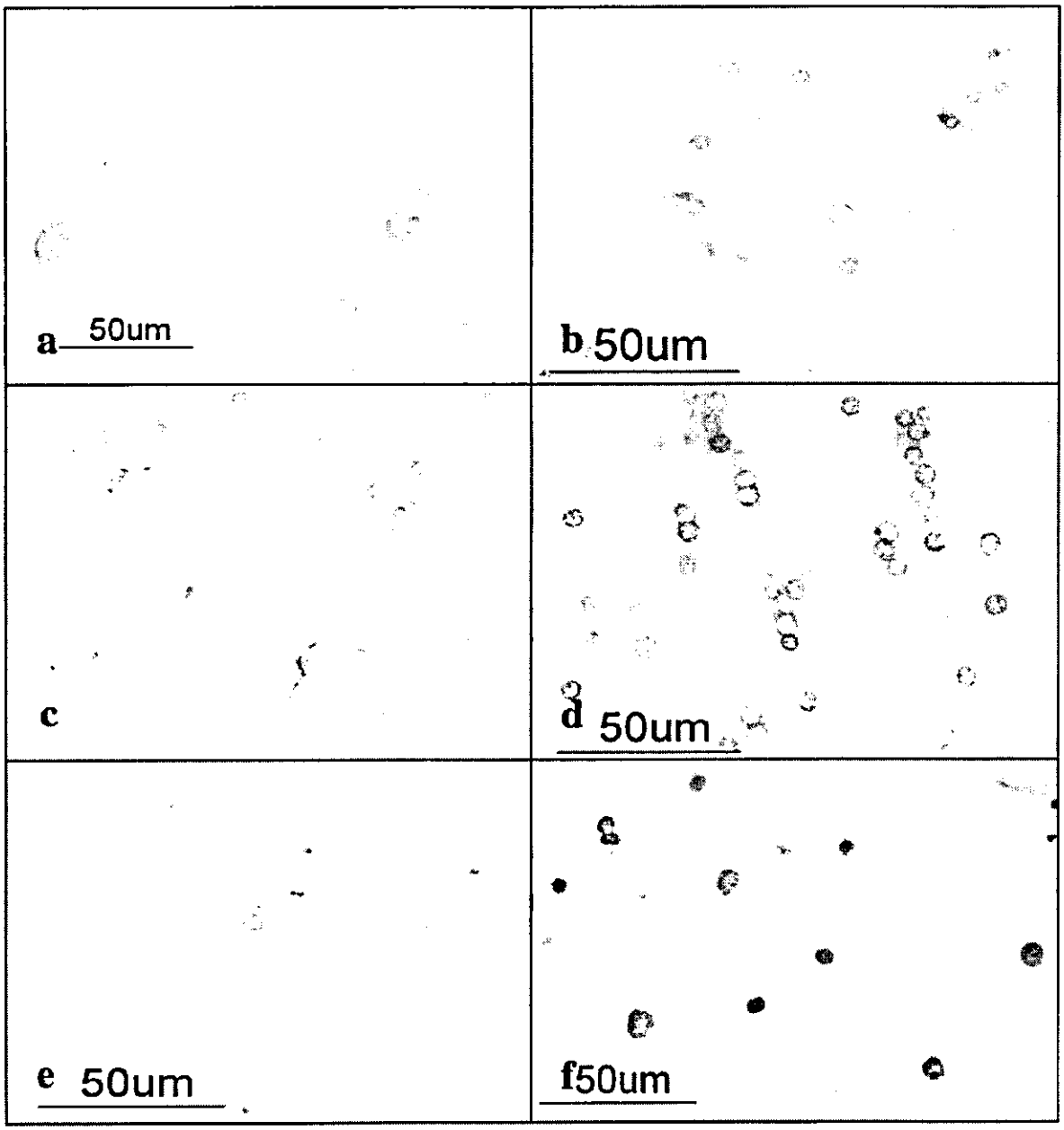

Figure 6. Expression of various 14-3-3 isoforms in neurons, astrocytes, oligodendrocytes, and microglia in non-MS brains. The brains of non-MS control cases were processed for immunohistochemical analysis using a battery of 14-3-3 isoform specific antibodies. **a** to **f** represent the following: **a:** no. 69 neurologically normal subject, the frontal cerebral cortex (×). Cortical neurons are stained. **b:** No. 523 schizophrenia, frontal cerebral cortex (×). Astrocytes are stained. **c:** No. 826 schizophrenia, the frontal cerebral cortex (×). Microglia are stained. **d:** No. 786 acute cerebral infarction, the subcortical white matter of the parietal lobe (×). Surviving oligodendrocytes are stained. **e:** No. 67 neurologically normal subject, the frontal cerebral cortex (×). A few astrocytes are stained. **f:** No. 789 old cerebral infarction, the frontal cerebral cortex (×). The nuclei of reactive astrocytes are stained.

lowed by centrifugation at 12,000 rpm at room temperature for 20 minutes. After preclearance, the supernatant was incubated at 4°C for 1 hour with a panel of anti-14-3-3 protein antibodies or the same amount of normal rabbit IgG (Santa Cruz Biotechnology). It was then incubated with Protein G Sepharose (Amersham Bioscience, Piscataway, NJ). After several washes, the immunoprecipitates were processed for Western blot analysis using V9 antibody or mouse monoclonal antibody against GFAP (GA5; Nichrei).

Two-Dimensional Gel Electrophoresis and Mass Spectrometry Analysis

To prepare total protein extract for two-dimensional gel electrophoretic analysis, the cells were homogenized in

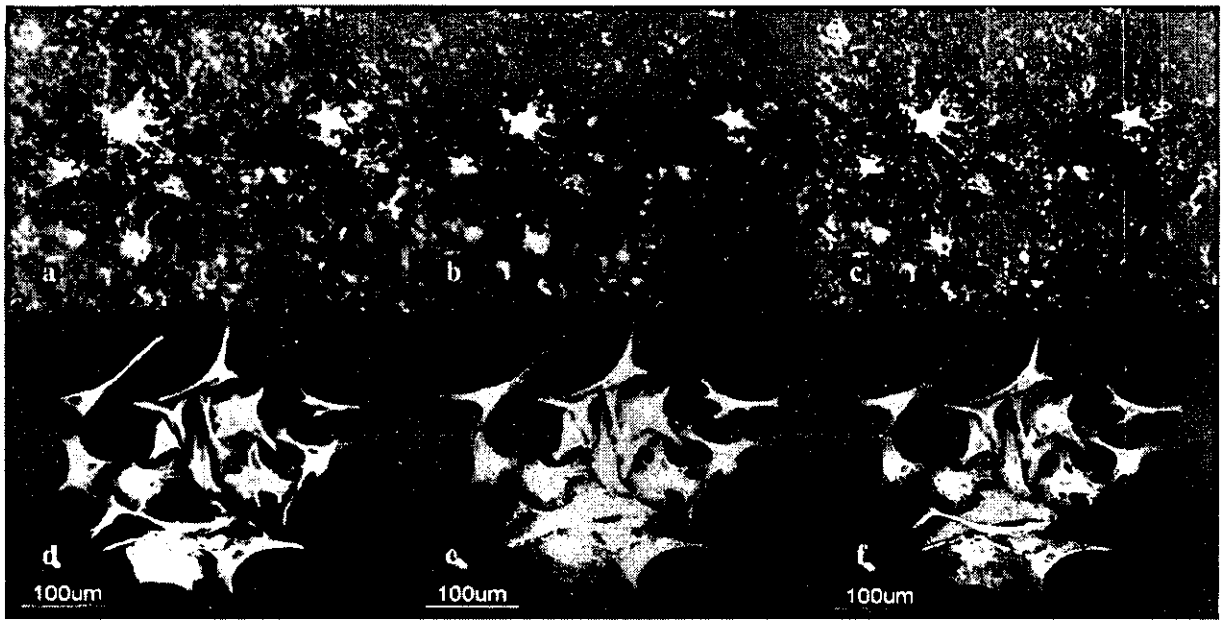

Figure 7. Co-expression of the 14-3-3ε isoform and GFAP in reactive astrocytes in chronic demyelinating lesions of MS and in cultured human astrocytes. Cultured human astrocytes and MS brain tissues were processed for double immunolabeling with anti-GFAP antibody and ε isoform-specific antibody followed by labeling with fluorescein isothiocyanate- and rhodamine-conjugated secondary antibodies. **a** to **f** represent no. 7-14, chronic active demyelinating lesions in the subcortical white matter of the frontal lobe (**a**–**c**), cultured human astrocytes (AS BW 1) (**d**–**f**). GFAP (**a**, **d**), ε (**b**, **e**), and the overlay (**c**, **f**).

rehydration buffer composed of 8 mol/L urea, 2% CHAPS, 0.5% carrier ampholytes (pH 4 to 6), 20 mmol/L dithiothreitol, 0.002% bromophenol blue, and a cocktail of protease inhibitors and phosphatase inhibitors (Sigma). Urea-soluble protein was separated by isoelectric focusing using the ZOOM IPGRunner system (Invitrogen) loaded with an immobilized pH 4.5 to 5.5 gradient strip. After the first dimension of isoelectric focusing, the protein was separated in the second dimension on a NuPAGE 4 to 12% polyacrylamide gel (Invitrogen). The gel was stained using Coomassie brilliant blue G-250 solution or the Silverquest silver staining kit (Invitrogen). It was transferred onto a polyvinylidene difluoride membrane for protein overlay and Western blot analysis. Spots of interest were excised from the gels, trypsinized, and processed for mass spectrometry (nanoESI-MS/MS) analysis followed by database searching using MASCOT software (Invitrogen Proteome, Yokohama, Japan).

Protein Overlay Analysis

To prepare the 14-3-3 protein-specific probe for protein overlay analysis, the open reading frame of the human 14-3-3ε isoform gene (YWHAE, GenBank accession No. NM_006761) was amplified from the cDNA of NTera2-N cells by the polymerase chain reaction using sense and anti-sense primers (5′atggatgatcgagaggatctggtg3′ and 5′tcactgattttcgtcttccacgtc3′). The polymerase chain reaction product was cloned into a prokaryotic expression vector pTrcHis-TOPO (Invitrogen). The expression of recombinant human 14-3-3ε protein having an N-terminal Xpress tag for detection (rh14-3-3ε) was induced in *Escherichia coli* by exposure to isopropyl β-thiogalactoside. The recombinant protein was further purified through a HiTrap chelating HP column (Amersham Bioscience) and by separation on a 12% SDS-PAGE gel. Recombinant human interferon-stimulated protein ISG15 fused to an N-terminal Xpress tag (rhISG15), a vimentin-binding protein in human cancer cells,[37] was prepared for the control probe. The polyvinylidene difluoride membrane on which the gel was blotted was incubated at room temperature overnight with 1 μg/ml rh14-3-3ε or rhISG15 probe, followed by immunolabeling with mouse monoclonal anti-Xpress antibody (Invitrogen) and horseradish peroxidase-conjugated anti-mouse IgG. After the probes and antibodies were stripped by incubating the membrane at 50°C for 30 minutes in stripping buffer, it was repeatedly relabeled with V9 antibody, GA5 antibody, or rabbit polyclonal antibodies specific for phosphorylated Ser-39, Ser-72, or Ser-83 epitopes of vimentin (Santa Cruz Biotechnology), followed by incubation with horseradish peroxidase-conjugated anti-mouse or rabbit IgG.

Results

Growth-Dependent Expression of 14-3-3 Isoforms in Cultured Human Astrocytes

To investigate the expression pattern of seven 14-3-3 isoforms in human neural cells, cultured human astrocytes, NTera2-N neurons, and U-373MG astrocytoma cells, all of which were incubated in 10% FBS-containing culture medium, were processed for Western blot analysis using a panel of isoform-specific antibodies or the antibodies broadly reactive against all of the isoforms listed in Table 1. Cultured human astrocytes, neurons, and astrocytoma cells, along with

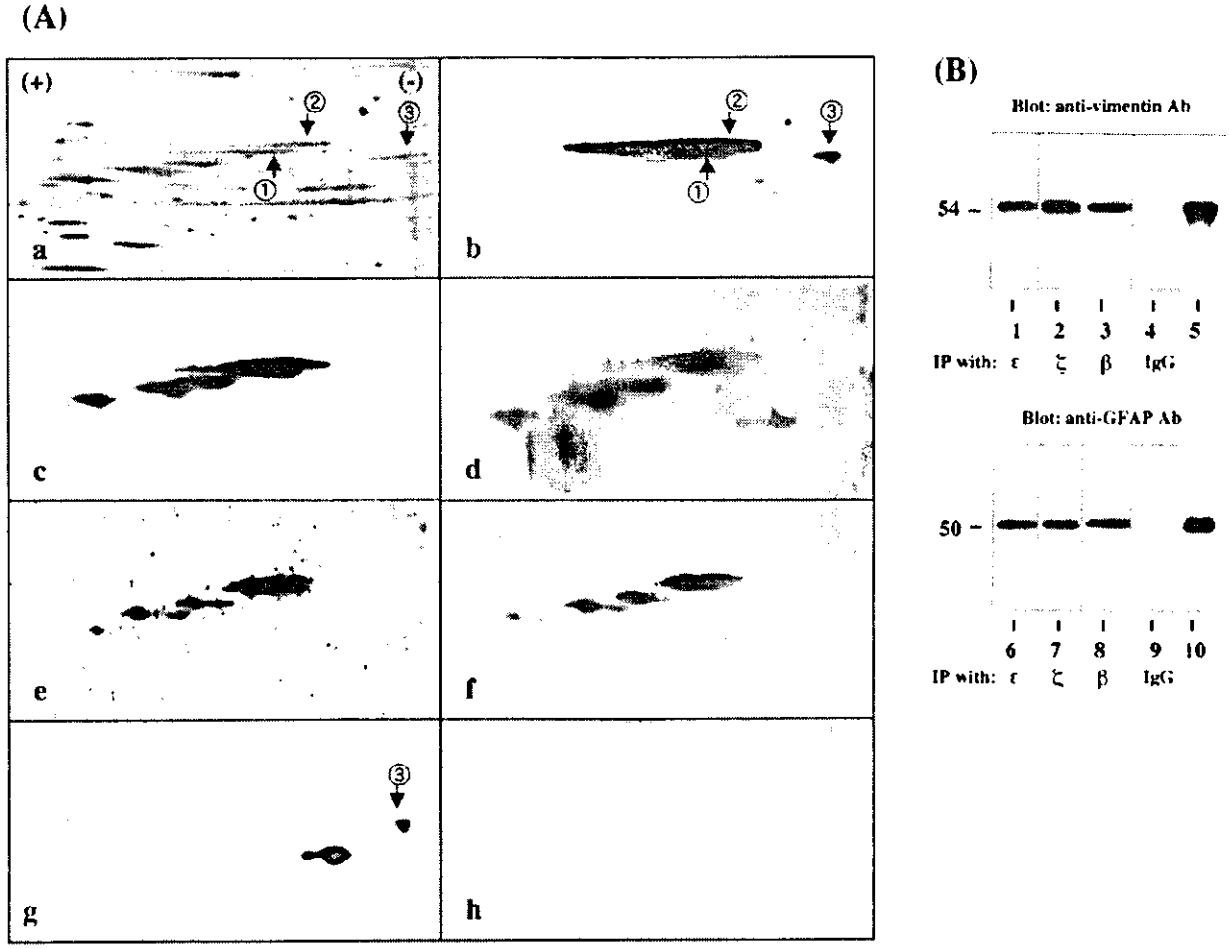

Figure 8. Two-dimensional gel electrophoresis and immunoprecipitation analysis of 14-3-3 ε isoform-binding proteins in cultured human astrocytes. **A:** Two-dimensional gel analysis. Human astrocytes (AS BW) were incubated in 10% FBS-containing culture medium. Twenty-one μg of total protein extract was separated on a two-dimensional PAGE gel, transblotted onto a polyvinylidene difluoride membrane, and processed for overlay analysis with recombinant human 14-3-3ε protein possessing the Xpress tag (rh14-3-3ε) followed by labeling with anti-Xpress antibody. After the probe and antibody were stripped, the blot was repeatedly relabeled six times with the antibodies against GFAP, vimentin, and vimentin with specific phosphorylated serine epitopes, and with recombinant human interferon-stimulated protein ISG15 having the Xpress tag (rhISG15). **a** to **g** represent silver staining (**a**), rh14-3-3ε labeling followed by staining with anti-Xpress antibody (**b**), vimentin (**c**), vimentin with phosphorylated Ser-39 (**d**), vimentin with phosphorylated Ser-72 (**e**), vimentin with phosphorylated Ser-83 (**f**), GFAP (**g**), and rhISG15 labeling followed by staining with anti-Xpress antibody (**h**). Two major spots labeled with rh14-3-3ε and anti-vimentin antibody are named spot no. 1 and no. 2, while a spot labeled with rh14-3-3ε and anti-GFAP antibody is designated spot no. 3. Spots no. 1 and no. 2 were excised from the gel and processed for mass spectrometry (MS) analysis. **B:** Immunoprecipitation analysis. Total protein extract of cultured human astrocytes was immunoprecipitated with ε isoform-specific antibody (**lanes 1** and **6**), ζ isoform-specific antibody (**lanes 2** and **7**), β isoform-specific antibody (**lanes 3** and **8**), with the same amount of normal rabbit IgG (**lanes 4** and **9**), or untreated with any antibodies (**lanes 5** and **10**; 2 μg of total protein extract before processing for immunoprecipitation). Then, the immunoprecipitates were processed for Western blot analysis using anti-vimentin (**top**) or anti-GFAP antibody (**bottom**).

human brain homogenate, expressed substantial levels of β, γ, ε, ζ, η, and θ isoforms (Figure 1, a to h; lanes 1 to 4). In contrast, the σ isoform was undetectable in human neural cells but was identified in HeLa cells (Figure 1i, lanes 1 to 5).

To study the effects of culture conditions on 14-3-3 protein levels, human astrocytes were incubated for 7 days in 10% FBS-containing culture medium or in the serum-free culture medium, which led to nearly complete growth arrest. The expression levels of β, γ, ε, ζ, η, and θ isoforms were elevated in human astrocytes incubated in the serum-containing growth-promoting condition. The expression was enhanced 3.3-, 1.6-, 2.2-, 10.0-, 18.7-, or 4.6-fold, respectively, compared with the levels under the serum-free growth-arrested condition when standardized against the levels of HSP60, a housekeeping gene product on the identical blots (Figure 2, a to c, e to g; top and bottom panels, lanes 1 and 2). The serum-induced up-regulation of 14-3-3 isoforms was also observed in a different culture of human astrocytes (Figure 2d, top and bottom panels, lanes 1 and 2) and mouse astrocytes in culture (Figure 2h, top and bottom panels, lanes 1 and 2; and additional data shown in Supplementary Figure 2 on The American Journal of Pathology website at *http://www.amjpathol.org*). These results indicate that cultured human astrocytes constitutively express all iso-

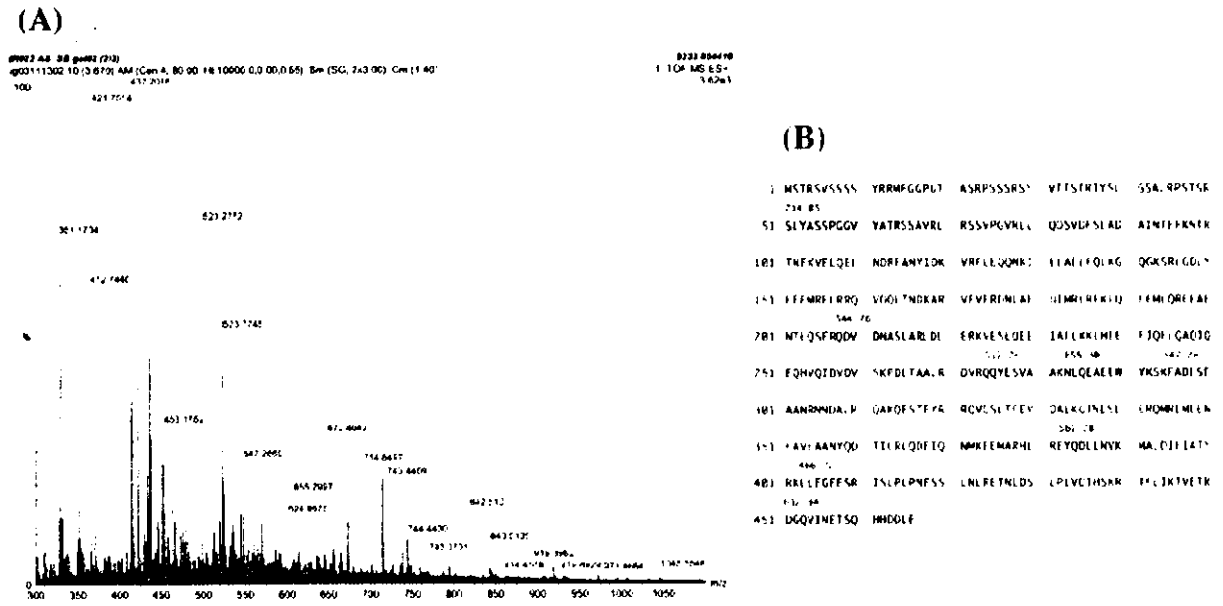

Figure 9. Mass spectrometry analysis of the 14-3-3ε isoform binding proteins in cultured human astrocytes. Spots no. 1 and no. 2 labeled with the rbl 14-3-3ε probe (Figure 8A, a and b) were excised from the gel, trypsinized, and processed for nanoESI MS/MS analysis. **A:** The spectra of nanoESI MS/MS analysis of spot no. 1. Each peak indicates individual peptide fragments. The position of several peaks was automatically numbered on the spectra. Peptides derived from the autolytic fragments of trypsin (eg, a12, a21, and 52,5) were omitted to be processed for further analysis. The peptide fragments were selected for MS analysis in order of their signal intensity. **B:** Amino acid sequence of human vimentin. Eight peptide fragments of spot no. 1 identified by nanoESI MS/MS analysis (**shadowed**) showed a perfect match with the amino acid sequence encompassing residues 51 to 466 of vimentin. The number indicated on each fragment represents the position in the horizontal axis of the spectra (**A**).

forms except for σ, whose levels were elevated in a cell growth-dependent manner.

Differential Expression of 14-3-3 Isoforms in Reactive Astrocytes in Demyelinating Lesions of MS

To investigate the differential expression of seven 14-3-3 isoforms in MS lesions, the brain, spinal cord, and optic nerve of four progressive MS patients (no. 791, no. 744, no. 609, and no. 544) and 12 non-MS control cases were processed for immunohistochemistry using a panel of isoform-specific antibodies. In chronic active and inactive demyelinating lesions of MS, the majority of GFAP$^+$ hypertrophic astrocytes intensely expressed β, ε, ζ, and η isoforms, whereas a small population of reactive astrocytes displayed immunoreactivities against γ, θ, and σ isoforms (Table 2; Figure 3, a to e; Figure 4 a and b). Reactive astrocytes immunoreactive against the 14-3-3 protein exhibited the most dense accumulation at the lesion edge, although they were widely distributed in demyelinating lesions and in the normal appearing white matter. A glial scar was also intensely labeled with the antibodies against β, ε, ζ, and η isoforms (ε shown in Figure 3e and the others not shown). In MS and non-MS brains, a major population of cerebral cortical neurons constitutively expressed high levels of β, γ, ζ, and η isoforms, and to a lessor degree, θ isoform, whereas they hardly showed immunoreactivity for the σ isoform, and a small population of cerebral cortical neurons in MS and non-MS brains occasionally expressed weak immunoreactivity for the ε isoform, although these findings varied among brains for different cases (Table 2; Figure 4, c to f; and Figure 6). Disrupted, distorted, and swollen axons found in the active demyelinating lesions of MS exhibited strong immunoreactivity against γ and ζ isoforms (γ shown in Figure 5a and the other not shown).

A very small population of reactive astrocytes in demyelinating lesions of MS, which occasionally showed a binucleated morphology, intensely expressed the σ isoform, whose expression was not detected in cultured human astrocytes (Figure 5c). A number of reactive astrocytes that appeared in the ischemic lesions of cerebral infarction expressed strong immunoreactivity against ε, ζ, and η isoforms (Table 2; Figure 5b), and the σ isoform was again strongly expressed in a very small number of reactive astrocytes (Figure 5d). The immunoreactivity against the η isoform was often concentrated in the nuclear region of reactive astrocytes in MS lesions (not shown) and the ischemic lesions (Figure 6; a to f). Furthermore, some GFAP$^+$ astrocytes occasionally identified in the brains of schizophrenia and neurologically normal patients expressed ε and σ isoforms at variable levels (Table 2; Figure 6, b and e). CD68$^+$ macrophages and microglia, with the greatest accumulation identified in the center and edge of active demyelinating lesions of MS and necrotic lesions of cerebral infarction, expressed β, ζ, and η isoforms, whereas they did not show substantial immunoreactivity against ε, θ, or σ isoforms (Table 2; Figure 6c). CD3$^+$ lymphocytes found in the perivascular cuffs of active MS lesions expressed variable immunoreactivities for β and ζ isoforms (not shown). A substantial

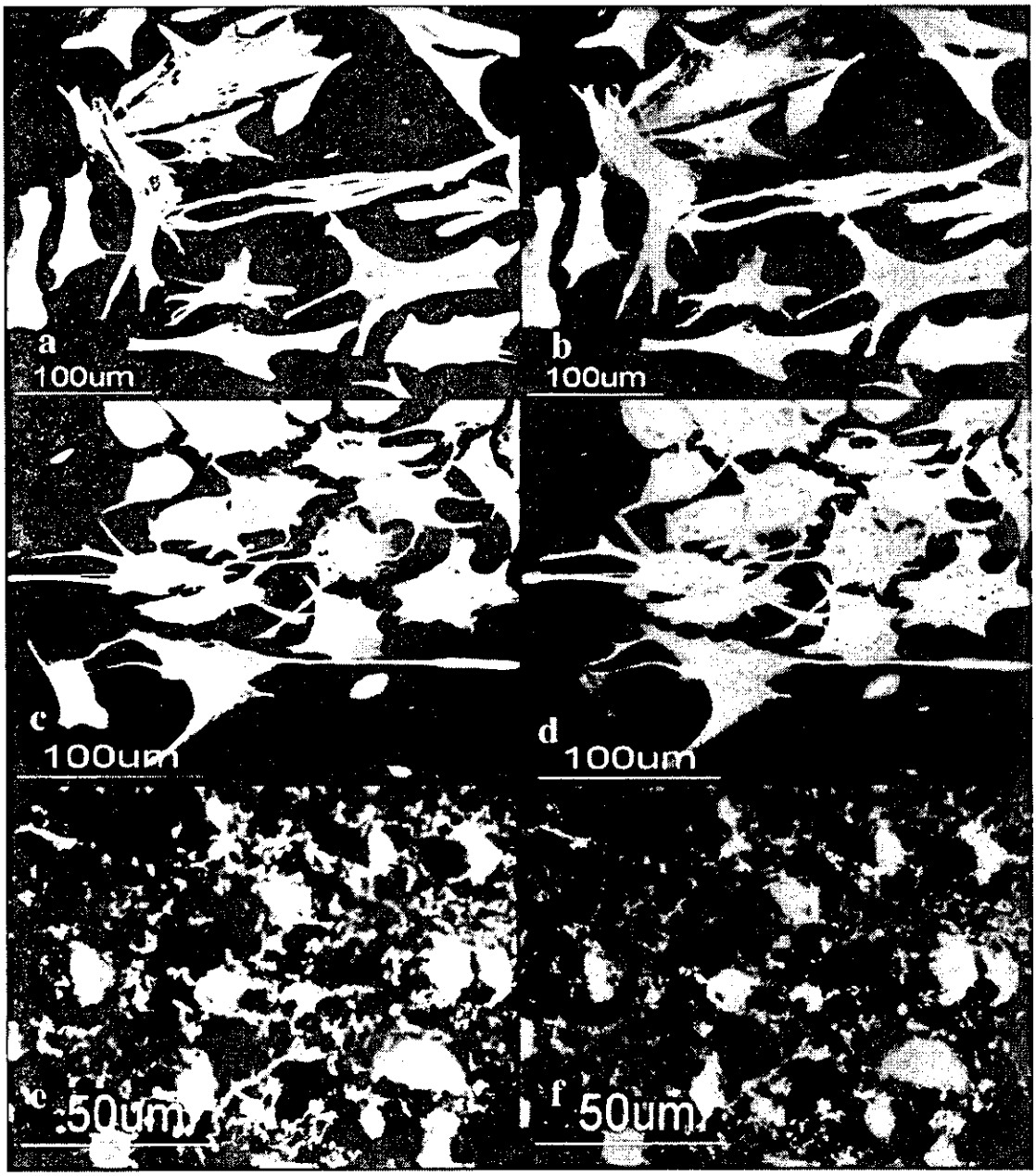

Figure 10. Co-expression of the 14-3-3 ε isoform and vimentin in cultured human astrocytes and reactive astrocytes in chronic demyelinating lesions of MS. Cultured human astrocytes and MS brain tissues were processed for double immunolabeling with anti vimentin antibody and ε isoform specific antibody or anti GFAP antibody followed by labeling with fluorescein isothiocyanate- and rhodamine-conjugated secondary antibodies. **a** to **f** represent cultured human astrocytes (AS BW1) (**a–d**); no. 744, chronic active demyelinating lesions in the subcortical white matter of the frontal lobe (**e**, **f**); vimentin (**a**, **c**, **e**); ε (**b**, **f**); and GFAP (**d**).

population of oligodendrocytes, which survived in chronic active demyelinating lesions of MS and ischemic lesions of cerebral infarction, expressed intense immunoreactivity against θ isoform (Table 2; Figure 5, e and f; and Figure 6d). These results suggest that markedly up-regulated expression of the ε isoform is the most reliable marker for identifying reactive astrocytes in MS and non-MS brains. Co-expression of the ε isoform and GFAP was verified in reactive astrocytes in MS lesions (Figure 7; a to c) and cultured human astrocytes (Figure 7; d to f) by double immunolabeling.

Binding of the 14-3-3ε Isoform to Vimentin and GFAP in Cultured Human Astrocytes

To identify the binding partner of the 14-3-3 protein in human astrocytes, we performed a protein overlay anal-

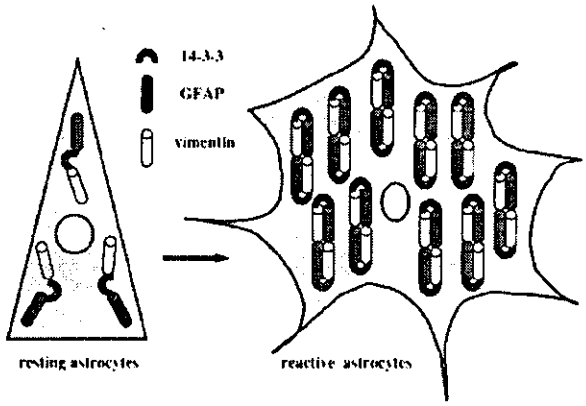

Figure 11. Putative role of the 14-3-3 protein in reactive gliosis in MS. Reactive gliosis is characterized by hypertrophy and proliferation of astrocytes associated with enhanced expression of GFAP (green) and vimentin (orange), which are co-polymerized in assembled filaments. Cultured human astrocytes expressed β, γ, ε, ζ, η, and θ isoforms, whose levels were markedly up-regulated under the growth promoting culture condition, in which the 14-3-3 protein (red) interacted with vimentin (orange) and GFAP (green). These observations suggest that the 14-3-3 protein (red) might act as an adaptor that connects vimentin (orange) and GFAP (green) in reactive astrocytes at the site of demyelinating lesions in MS.

ysis using recombinant human 14-3-3ε protein with the Xpress tag (rh14-3-3ε) as a probe. Human astrocytes were incubated in 10% FBS-containing culture medium. Total protein extract was separated on a two-dimensional PAGE gel (Figure 8A, a) and transferred onto a polyvinylidene difluoride membrane (Figure 8A, b to h). The rh14-3-3ε probe strongly reacted with several spots on the blot, among which two major 54-kd spots were designated spots no. 1 and no. 2 (Figure 8A, b). In contrast, the rhISG15 probe did not react with these spots, excluding nonspecific binding of rh14-3-3ε via the Xpress tag (Figure 8A, h). Spots no. 1 and no. 2 were excised from the original gels, trypsinized, and processed for nanoESI-MS/MS analysis (Figure 9A). Among the peaks detected, eight peptide fragments derived from spot no. 1 and six from spot no. 2 showed a perfect match with the amino acid sequence covering residues 51 to 466 of human vimentin (Figure 9B), suggesting that these spots correspond to nearly full-length vimentin. Intense vimentin immunoreactivity was also identified in reactive astrocytes in demyelinating lesions of MS (Figure 3f). Furthermore, anti-vimentin monoclonal antibody reacted with spots no. 1 and no. 2, although this antibody labeled three additional, more acidic spots having smaller molecular weights (Figure 8A, c). The latter might represent post-translationally modified isoforms or degradation products of vimentin. Because vimentin is heavily phosphorylated at multiple serine residues in various mesenchymal cells, the phosphorylation state was characterized by repeated relabeling of the blot with three different antibodies specific for phosphorylated serine epitopes of vimentin. Phosphorylated Ser-39-, Ser-72-, and Ser-83-specific antibodies strongly reacted with spots no. 1 and no. 2, along with three additional spots unlabeled with rh14-3-3ε, suggesting that these serine residues are not involved in the interaction of the ε isoform with vimentin (Figure 8A, d to f). Protein overlay analysis using the rh14-3-3ε probe identified a distinct spot, designated spot no. 3 (Figure 8A, b). This spot was labeled with anti-GFAP antibody, indicating that GFAP is another binding partner of the 14-3-3 protein (Figure 8A, g). A more acidic spot having a smaller molecular weight immunoreactive for GFAP and weakly labeled with rh14-3-3ε might represent a post-translationally modified isoform or a degradation product of GFAP (Figure 8A, b and g). Vimentin and GFAP were detected in the immunoprecipitates of cultured human astrocyte protein extract, when the lysate was incubated with the ε, β, or ζ isoform-specific antibody (Figure 8B, top and bottom panels, lanes 1 to 3, 6 to 8). In contrast, only marginal bands were found in those with normal rabbit IgG (Figure 8B, top and bottom panels, lanes 4 and 9). Co-expression of the ε isoform with vimentin and GFAP was verified in cultured human astrocytes (Figure 10, a to d) and in reactive astrocytes in demyelinating lesions of MS (Figure 10, e and f) by double immunolabeling.

Discussion

The present study showed that seven 14-3-3 isoforms are differentially expressed in reactive astrocytes in demyelinating lesions of MS. Human astrocytes in culture also expressed β, γ, ε, ζ, η, and θ isoforms whose levels were markedly elevated under the growth-promoting culture condition. In demyelinating lesions of MS, the majority of GFAP$^+$ hypertrophic astrocytes intensely expressed β, ε, ζ, and η isoforms, although the expression of these isoforms was found in reactive astrocytes appearing in non-MS brains. Previous studies showed that the σ isoform expression is confined to differentiated squamous epithelial cells.[19,31] However, we found that some reactive astrocytes in MS and non-MS brains intensely expressed this isoform. Neurons constitutively expressed β, γ, ζ, and η isoforms but they did not constantly express ε or σ isoforms. Macrophages and microglia in MS and non-MS lesions intensely expressed β, ζ, and η isoforms, but they did not express ε, θ, or σ isoforms. A substantial population of oligodendrocytes, surviving in active demyelinating lesions of MS and ischemic lesions of cerebral infarction, intensely expressed the θ isoform, consistent with the expression of this isoform in the white matter of the developing rat CNS.[7] These observations are in agreement with our previous findings that the 14-3-3 protein is expressed not only in neurons but also in astrocytes, microglia, and oligodendrocytes in mouse brain cell cultures.[26] The present observations suggest that up-regulated expression of the ε isoform could be used as an immunohistochemical marker to identify reactive astrocytes at least in demyelinating lesions of MS and ischemic lesions of cerebral infarction. However, Lewy bodies in the Parkinson's disease brain[30] and a minor population of neurons in MS and non-MS brains express the ε isoform, indicating that this isoform is not astrocyte-specific.

The biological role of ε and σ isoforms in human astrocyte function remains unknown. Increasing evidence indicates that isoform-specific function regulates the devel-

opment and differentiation of neural and nonneural cells. Particularly, the ϵ isoform plays a role in the regulation of various cellular signaling events. The 14-3-3ϵ gene is deleted in the patients with Miller-Dieker syndrome, a human neuronal migration disorder presenting with the most severe form of lissencephaly (LIS) associated with facial abnormalities.[39] ϵ Isoform-deficient mice are defective in neuronal migration during brain development.[40] The multimolecular complex composed of the ϵ isoform, LIS1 and nudE nuclear distribution gene E homolog-like 1 (NUDEL) regulates the activity of dynein, a cytoplasmic motor protein, suggesting a role of ϵ in neuronal migration.[40] Somatic homozygous deletion of the 14-3-3ϵ gene is frequently found in small cell lung cancers, supporting the idea that the ϵ isoform serves as a tumor suppressor gene.[41] The 14-3-3ϵ isoform, by binding to the intracellular domain of the p75 neurotrophin receptor (NTR) in a NGF-dependent manner, promotes p75NTR-associated cell death executor (NADE)-mediated apoptosis.[42] During apoptosis, the ϵ protein is cleaved by caspase-3 at a cleavage site located in the C-terminal hydrophobic tail, where the amino acid sequence is highly variable among different 14-3-3 isoforms.[43] The ϵ isoform interacts with cdc25A and cdc25B phosphatases, key enzymes required for cell-cycle progression by activating cyclin-dependent kinases.[44] Phosphorylation-dependent interaction of the ϵ isoform with heat shock transcription factor HSF1 restricts the location of HSF1 in the cytoplasm by keeping it in an inactive form.[45] The ϵ isoform catalyzes the depolymerization and unfolding of mitochondrial precursor proteins in an ATP-dependent manner.[46] Based on these observations, we propose that the ϵ isoform plays a regulatory role in proliferation, apoptosis, and stress responses in reactive astrocytes.

The σ isoform constitutes a component of the G_2/M cell-cycle checkpoint machinery.[47] Exposure of the cells to DNA-damaging agents results in p53-dependent induction of the σ isoform, which in turn arrests the cells in the G_2/M phase by sequestering the cdc2-cyclin B1 complex in the cytoplasm.[48] Therefore, σ isoform-deficient cells are unable to maintain cell-cycle arrest.[47] Selective down-regulation of the σ isoform because of the hypermethylation of CpG islands in its promoter region is responsible for the malignant transformation of breast cancer cells,[49] whereas reduced expression of the σ isoform allows human epidermal keratinocytes to escape replicative senescence.[50] These observations raise the possibility that a population of reactive astrocytes with strong immunoreactivity against the σ isoform might represent the cells responding to DNA damage at the site of demyelinating lesions in MS and ischemic lesions of cerebral infarction.

Reactive gliosis is characterized by hypertrophy and proliferation of astrocytes associated with enhanced expression of GFAP and vimentin, accompanied by increased production of growth factors, cytokines, neuropeptides, and extracellular matrix molecules.[51,52] Astrocytes play a role in the repair of the blood-brain barrier, protection of neurons from glutamate excitotoxicity, and enhancement of neuronal survival by supplying neurotrophic factors.[53] On the other hand, reactive astrocytes strongly inhibit neurite outgrowth by forming glial scars after CNS injury and inflammation.[53,54] Through protein overlay and nanoESI-MS/MS analysis, we showed that vimentin is the major 14-3-3 protein-interacting protein expressed in cultured human astrocytes. Consistent with previous observations,[55,56] we identified vimentin expression in reactive astrocytes in demyelinating lesions of MS. Astrocytes isolated from vimentin-deficient mice possess an abnormal filamentous network of GFAP.[57,58] Furthermore, mice lacking vimentin and GFAP do not form proper glial scars after CNS injury, indicating that the type III IF family proteins play a pivotal role in cytoskeletal organization in astrocytes.[59]

In our study, the rh14-3-3ϵ probe strongly reacted with two distinct spots named no. 1 and no. 2 among five phosphovimentin-immunoreactive spots on the blot. Vimentin was immunoprecipitated with the ζ and β isoforms along with ϵ. These observations suggest that the interaction between vimentin and the 14-3-3 protein is not isoform-specific, and that the 14-3-3 protein-binding domain in vimentin might not include phosphorylated Ser-39, Ser-72, and Ser-83 epitopes. Protein overlay analysis identified GFAP as another binding partner of the 14-3-3ϵ isoform. Immunoprecipitation experiments verified the interaction between GFAP and the ϵ, ζ, or β isoform. However, a different spot strongly immunoreactive against GFAP but much weakly labeled with rh14-3-3ϵ was identified on the two-dimensional gel blot. This suggests that a substantial pool of cytoplasmic vimentin and GFAP proteins steadily interact with the 14-3-3 protein in human astrocytes.

Our observations raise the possibility that the 14-3-3 protein acts as an adaptor that connects vimentin and GFAP in cultured human astrocytes (Figure 11). Previous studies showed that vimentin and GFAP are co-expressed and co-polymerized in assembled filaments in astrocytes,[55,60] supporting the view that the 14-3-3 protein not only bridges vimentin and GFAP one by one, but also bundles both of them in the same assembled filaments. All these proteins are expressed at much higher levels in reactive astrocytes, which require more efforts to coordinate the IF network compared with resting astrocytes (Figure 11). Several other binding partner candidates for vimentin in astrocytes include α-crystallin, which inhibits the *in vitro* assembly of GFAP,[61] and the multiple endocrine neoplasia type 1 (MEN1) gene product named menin, which binds to vimentin and GFAP in glioma cells.[62] The 14-3-3γ isoform interacts with F-actin and Raf kinase in cultured mouse astrocytes, indicating its role in cytoskeletal rearrangement during cell growth and division.[63,64] Importantly, a recent study using COS-7 cells overexpressing the 14-3-3 protein showed that phosphorylated vimentin binds to the 14-3-3 protein and limits the interaction of 14-3-3 with other 14-3-3-binding partners, thereby modulating Raf-dependent intracellular signaling.[65] This study also found that vimentin does not have typical consensus 14-3-3-binding motifs.[65] However, a close interaction of the 14-3-3 protein with phosphorylated vimentin affects the phosphorylation and dephosphorylation state of vimentin.[65] Site-specific phosphorylation of vimentin and GFAP is mediated by

a range of protein kinases, including Rho kinase, cdc2 kinase, Ca^{2+} calmodulin-dependent kinase II, protein kinases A and C, and Aurora-B kinase.[60,66–69] They coordinately regulate dynamic equilibrium between the assembly and disassembly of IF proteins during mitosis.[60,66–69] Furthermore, these kinases are identified as binding partners for the 14-3-3 protein.[1–3] Therefore, our observations suggest that the 14-3-3 protein plays a role in the organization of IF proteins and IF-related kinases during conversion from resting astrocytes to reactive astrocytes. A role for 14-3-3 protein in IF dynamics is supported by our preliminary observations that suggest the effects of difopein,[70] a specific inhibitor of 14-3-3 protein/ligand interaction, on the morphological characteristics of cultured human astrocytes.

Acknowledgments

We thank Dr. Mitsuru Kawai, Department of Neurology, National Center Hospital for Mental, Nervous, and Muscular Disorders, NCNP, Tokyo, Japan, for providing information about MS patients; Dr. Toshikazu Murakami, Department of Pathology, Kohnodai Hospital, NCNP, Chiba, Japan, for providing the brains of neurologically normal controls; Drs. Kazuhiko Watabe and S.U. Kim, University of British Columbia, Vancouver, BC, Canada, for providing cultured fetal human astrocytes; and Dr. Masashi Fukuda, Invitrogen Proteome, Yokohama, Japan, for his help in nanoESI-MS/MS analysis.

References

1. Fu H, Subramanian RR, Masters SC: 14-3-3 proteins: structure, function, and regulation. Annu Rev Pharmacol Toxicol 2000, 40:617–647
2. van Hemert MJ, Steensma HY, van Heusden GPH: 14-3-3 proteins: key regulators of cell division, signalling and apoptosis. Bioessays 2001, 23:936–946
3. Aitken A, Baxter H, Dubois T, Clokie S, Mackie S, Mitchell K, Peden A, Zemlickova E: 14-3-3 proteins in cell regulation. Biochem Soc Trans 2002, 30:351–360
4. Berg D, Holzmann C, Riess O: 14-3-3 proteins in the nervous system. Nature Rev Neurosci 2002, 4:752–762
5. Boston PF, Jackson P, Kyonoch PAM, Thompson RJ: Purification, properties, and immunohistochemical localisation of human brain 14-3-3 protein. J Neurochem 1982, 38:1466–1474
6. Watanabe M, Isobe T, Ichimura T, Kuwano R, Takahashi Y, Kondo H: Molecular cloning of rat cDNAs for β and γ subtypes of 14-3-3 protein and developmental changes in expression of their mRNAs in the nervous system. Mol Brain Res 1993, 17:135–146
7. Watanabe M, Isobe T, Ichimura T, Kuwano R, Takahashi Y, Kondo H, Inoue Y: Molecular cloning of rat cDNAs for the ζ and θ subtypes of 14-3-3 protein and differential distributions of their mRNAs in the brain. Mol Brain Res 1994, 25:113–121
8. Muslin AJ, Xing H: 14-3-3 proteins: regulation of subcellular localization by molecular interference. Cell Signal 2000, 12:703–709
9. Yaffe MB: How do 14-3-3 proteins work? Gatekeeper phosphorylation and the molecular anvil hypothesis. FEBS Lett 2002, 513:53–57
10. Tzivion G, Avruch J: 14-3-3 proteins: active cofactors in cellular regulation by serine/threonine phosphorylation. J Biol Chem 2002, 277:3061–3064
11. Zhai J, Lin H, Shamim M, Schlaepfer WW, Canoll P, Sole R: Identification of a novel interaction of 14-3-3 with p190RhoGEF. J Biol Chem 2001, 276:41318–41324
12. Dai J G, Murakami K: Constitutively and autonomously active protein kinase C associated with 14-3-3 ζ in the rodent brain. J Neurochem 2003, 84:23–34
13. Broadie K, Rushton E, Skoulakis EMC, Davis RL: Leonardo, a Drosphila 14-3-3 protein involved in learning, regulates presynaptic function. Neuron 1997, 19:391–402
14. Meller N, Liu Y C, Collins II, Bonnefoy Bérard N, Naief G, Isakov N, Altman A: Direct interaction between protein kinase Cθ (PKCθ) and 14-3-3τ in T cells: 14-3-3 overexpression results in inhibition of PKCθ translocation and function. Mol Cell Biol 1996, 16:5782–5791
15. Craparo A, Freund R, Gustafson TA: 14-3-3 (ε) interacts with the insulin-like growth factor I receptor and insulin receptor substrate I in a phosphoserine-dependent manner. J Biol Chem 1997, 272:11663–11669
16. Vincenz C, Dixit VM: 14-3-3 proteins associate with A20 in an isoform-specific manner and function both as chaperone and adaptor molecules. J Biol Chem 1996, 271:20029–20034
17. Wakui H, Wright APH, Gustafsson J A, Zilliacus J: Interaction of the ligand-activated glucocorticoid receptor with the 14-3-3ζ/δ protein. J Biol Chem 1997, 272:8153–8156
18. Hashiguchi M, Sobue K, Paudel HK: 14-3-3ζ is an effector of tau protein phosphorylation. J Biol Chem 2000, 275:25247–25254
19. Lelders H, Madsen P, Rasmussen HH, Honoré B, Andersen AH, Walbum I, Vandekerckhove J, Celis JE: Molecular cloning and expression of the transformation sensitive epithelial marker stratifin: A member of a protein family that has been involved in the protein kinase C signaling pathway. J Mol Biol 1993, 231:982–998
20. Martin H, Rostas J, Patel Y, Aitken A: Subcellular localisation of 14-3-3 isoforms in rat brain using specific antibodies. J Neurochem 1994, 63:2259–2268
21. Baxter HC, Liu W G, Forster JL, Aitken A, Fraser JR: Immunolocalisation of 14-3-3 isoforms in normal and scrapie-infected murine brain. Neuroscience 2002, 109:5–14
22. Hsich G, Kenney K, Gibbs Jr CJ, Lee KH, Harrington MG: The 14-3-3 brain protein in cerebrospinal fluid as a marker for transmissible spongiform encephalopathies. N Engl J Med 1996, 335:924–930
23. Zerr I, Bodemer M, Gefeller O, Otto M, Poser S, Wiltfang J, Windl O, Kretzschmar HA, Weber T: Detection of 14-3-3 protein in the cerebrospinal fluid supports the diagnosis of Creutzfeldt-Jakob disease. Ann Neurol 1998, 43:32–40
24. Wiltfang J, Otto M, Baxter HC, Bodemer M, Steinacker P, Baldeweg T, Zerr I, Kornhuber J, Kretzschmar HA, Poser S, Hüther L, Aitken A: Isoform pattern of 14-3-3 proteins in the cerebrospinal fluid of patients with Creutzfeldt-Jakob disease. J Neurochem 1999, 73:2489–2490
25. Richard M, Biacabe A G, Strachenbergen N, Ironside JW, Mohr M, Kopp N, Perret-Liaudet A: Immunohistochemical localization of 14-3-3 ζ protein in amyloid plaques in human spongiform encephalopathies. Acta Neuropathol 2003, 105:296–302
26. Satoh J, Kurohara K, Yukitake M, Kuroda Y: The 14-3-3 protein detectable in the cerebrospinal fluid of patients with prion-unrelated neurological diseases is expressed constitutively in neurons and glial cells in culture. J Neurol 1999, 41:216–225
27. Satoh J, Yukitake M, Kurohara K, Takashima H, Kuroda Y: Detection of the 14-3-3 protein in the cerebrospinal fluid of Japanese multiple sclerosis patients presenting with severe myelitis. J Neurol Sci 2003, 212:11–20
28. Layfield R, Fergusson J, Aitken A, Lowe J, Landon M, Mayer RJ: Neurofibrillary tangles of Alzheimer's disease brains contain 14-3-3 proteins. Neurosci Lett 1996, 209:57–60
29. Agarwal-Mawal A, Qureshi HY, Cafferty PW, Yuan Z, Han D, Lin R, Paudel HK: 14-3-3 connects glycogen synthase kinase-3β to tau within a brain microtubule-associated tau phosphorylation complex. J Biol Chem 2003, 278:12722–12728
30. Berg D, Riess O, Bonnemann A: Specification of 14-3-3 proteins in Lewy bodies. Ann Neurol 2003, 54:135
31. Ostrerova N, Petrucelli L, Farrer M, Mehta N, Choi P, Hardy J, Wolozin B: α-Synuclein shares physical and functional homology with 14-3-3 proteins. J Neurosci 1999, 19:5782–5791
32. Xu J, Kao S Y, Lee FJS, Song W, Jin L W, Yankner BA: Dopamine-dependent neurotoxicity of α-synuclein: a mechanism for selective neurodegeneration in Parkinson disease. Nat Med 2002, 8:600–606
33. Chen H K, Fernandez-Funez P, Acevedo SF, Lam YC, Kaytor MD, Fernandez MH, Aitken A, Skoulakis EMC, Orr HT, Botas J, Zoghbi HY: Interaction of Akt-phosphorylated ataxin-1 with 14-3-3 mediates neurodegeneration in spinocerebellar ataxia type 1. Cell 2003, 113:457–468

34 Malaspina A, Kaushik N, de Belleroche J. A 14-3-3 mRNA is up-regulated in amyotrophic lateral sclerosis spinal cord. J Neurochem 2000, 75:2511–2520
35 Carpenter MK, Cui X, Hu ZY, Jackson J, Sherman S, Seiger A, Wahlberg LU. In vitro expansion of a multipotent population of human neural progenitor cells. Exp Neurol 1999, 158:265–278
36 Satoh J, Kuroda Y. Differential gene expression between human neurons and neuronal progenitor cells in culture: an analysis of arrayed cDNA clones in NTera2 human embryonal carcinoma cell line as a model system. J Neurosci Methods 2000, 94:155–164
37 Loeb KR, Haas AL. Conjugates of ubiquitin cross-reactive protein distribute in a cytoskeletal pattern. Mol Cell Biol 1994, 14:8408–8419
38 Prasad GL, Valverius EM, McDuffie E, Cooper HL. Complementary DNA cloning of a novel epithelial cell marker protein, HME1, that may be down-regulated in neoplastic mammary cells. Cell Growth Differ 1992, 3:507–513
39 Cardoso C, Leventer RJ, Ward HL, Toyo-oka K, Chung J, Gross A, Martin CL, Allanson J, Pilz DT, Olney AH, Mutchinick OM, Hirotsune S, Wynshaw-Boris A, Dobyns WB, Lodhotter DH. Refinement of a 400-kb critical region allows genotypic differentiation between isolated lissencephaly, Miller-Dieker syndrome, and other phenotypes secondary to deletions of 17p13.3. Am J Hum Genet 2003, 72:918–930
40 Toyo-Oka K, Shimoya A, Gambello MJ, Cardoso C, Leventer R, Ward HL, Ayala R, Tsai LH, Dobyns W, Ledbetter D, Hirotsune S, Wynshaw-Boris A. 14-3-3ε is important for neuronal migration by binding to NUDEL: a molecular explanation for Miller-Dieker syndrome. Nat Genet 2003, 34:274–285
41 Konishi H, Nakagawa T, Hanano T, Mizuno K, Saito H, Masuda A, Matsuda H, Osada H, Takahashi E. Identification of frequent G2 checkpoint impairment and a homozygous deletion of 14-3-3ε at 17p13.3 in small cell lung cancers. Cancer Res 2002, 62:271–276
42 Kimura M, Ito S, Shoji-Hoshino S, Mukai J, Nadano D, Oshimura M, Sato TA. 14-3-3 is involved in p75 neurotrophin receptor-mediated signal transduction. J Biol Chem 2001, 276:17291–17300
43 Won J, Kim DY, La M, Kim D, Meadows GG, Joe CO. Cleavage of 14-3-3 protein by caspase-3 facilitates Bad interaction with Bcl-x(L) during apoptosis. J Biol Chem 2003, 278:19347–19351
44 Conklin DS, Galaktionow K, Beach D. 14-3-3 proteins associate with cdc25 phosphatases. Proc Natl Acad Sci USA 1995, 92:7892–7896
45 Wang X, Grammatikakis N, Siganou A, Calderwood SK. Regulation of molecular chaperone gene transcription involves the serine phosphorylation, 14-3-3ε binding, and cytoplasmic sequestration of heat shock factor 1. Mol Cell Biol 2003, 23:6013–6026
46 Alam R, Hachiya N, Sakaguchi M, Kawabata S-I, Iwanaga S, Kitagawa M, Mihara K, Omura T. cDNA cloning and characterization of mitochondrial import stimulation factor (MSF) purified from rat liver cytosol. J Biochem 1994, 116:416–425
47 Chan TA, Hermeking H, Lengauer C, Kinzler KW, Vogelstein B. 14-3-3σ is required to prevent mitotic catastrophe after DNA damage. Nature 1999, 401:616–620
48 Hermeking H, Lengauer C, Polyak K, He TC, Zhang L, Thiagalingam S, Kinzler KW, Vogelstein B. 14-3-3σ is a p53-regulated inhibitor of G2/M progression. Mol Cell 1997, 1:3–11
49 Ferguson AT, Evron E, Umbricht CB, Pandita TK, Chan TA, Hermeking H, Marks JR, Lambers AR, Futreal PA, Stampfer MR, Sukumar S. High frequency of hypermethylation at the 14-3-3σ locus leads to gene silencing in breast cancer. Proc Natl Acad Sci USA 2000, 97:6049–6054
50 Dellambra E, Golisano O, Bondanza S, Siviero E, Lacal P, Molinari M, D'Atri S, De Luca M. Downregulation of 14-3-3σ prevents clonal evolution and leads to immortalization of primary human keratinocytes. J Cell Biol 2000, 149:1117–1129
51 Mucke L, Eddleston M. Astrocytes in infectious and immune-mediated diseases of the central nervous system. FASEB J 1993, 7:1226–1232
52 Ridet JL, Malhotra SK, Privat A, Gage FH. Reactive astrocytes: cellular and molecular cues to biological function. Trends Neurosci 1997, 20:570–577
53 Rush RG, Puvanachandra N, Horner CH, Polito A, Ostenfeld T, Svendsen CN, Mucke L, Johnson MH, Sofroniew MV. Leukocyte infiltration, neuronal degeneration, and neurite outgrowth after ablation of scar-forming, reactive astrocytes in adult transgenic mice. Neuron 1999, 23:297–308
54 Menet V, Prieto M, Privat A, Gibaja M. Annoy J, Colucci-Guyon E, Privat A. Inactivation of the glial fibrillary acidic protein gene, but not that of vimentin, improves neuronal survival and neurite growth by modifying adhesion molecule expression. J Neurosci 2001, 21:6174–6188
55 Yamada T, Kawamata T, Walker DG, McGeer PL. Vimentin immunoreactivity in normal and pathological human brain tissues. Acta Neuropathol 1992, 84:157–162
56 Holley JE, Gveric D, Newcombe J, Cuzner ML, Gutowski NJ. Astrocyte characterization in the multiple sclerosis glial scar. Neuropathol Appl Neurobiol 2003, 29:434–444
57 Galou M, Colucci-Guyon E, Ensergueix D, Ridet JL, Roberts MGY, Privat A, Babinet C, Dupouey P. Disrupted glial fibrillary acidic protein network in astrocytes from vimentin knockout mice. J Cell Biol 1996, 133:853–863
58 Hisanaga S, Sahlgren C, Botthold CH, Stakeborg J, Celis JE, Betsholtz C, Eriksson JE, Pekny M. Intermediate filament protein partnership in astrocytes. J Biol Chem 1999, 274:23996–24006
59 Pekny M, Johansson B, Hisanaga S, Stakeborg J, Wallen A, Perlmann T, Eriksson U, Betsholtz C, Berthold CH, Eriksson J. Abnormal reaction to central nervous system injury in mice lacking glial fibrillary acidic protein and vimentin. J Cell Biol 1999, 145:503–514
60 Inagaki M, Nakamura Y, Takeda M, Nishimura T, Inagaki N. Glial fibrillary acidic protein: dynamic property and regulation by phosphorylation. Brain Pathol 1994, 4:239–243
61 Nicholl ID, Quinlan RA. Chaperone activity of α-crystallins modulates intermediate filament assembly. EMBO J 1994, 13:945–953
62 Lopez-Egido JR, Cunningham J, Berg M, Oberg K, Bongcam-Rudloff E, Gobl AE. Menin's interaction with glial fibrillary acidic protein and vimentin suggests a role for the intermediate filament network in regulating menin activity. Exp Cell Biol 2002, 278:175–183
63 Chen XQ, Yu ACH. The association of 14-3-3γ and actin plays a role in cell division and apoptosis in astrocytes. Biochem Biophys Res Commun 2002, 296:657–663
64 Chen XQ, Chen JG, Zhang Y, Hsiao WWL, Yu ACH. 14-3-3γ is up-regulated by in vitro ischemia and binds to protein kinase Raf in primary cultures of astrocytes. Glia 2003, 42:315–324
65 Tzivion G, Luo Z-J, Avruch J. Calyculin A-induced vimentin phosphorylation sequesters 14-3-3 and displaces other 14-3-3 partners in vivo. J Biol Chem 2000, 275:29772–29778
66 Tsujimura K, Tanaka J, Ando S, Matsuoka Y, Kusubata M, Sugiura H, Yamauchi T, Inagaki M. Identification of phosphorylation sites on glial fibrillary acidic protein for cdc2 kinase and Ca2+/calmodulin-dependent protein kinase II. J Biochem 1994, 116:426–434
67 Goto H, Kosako H, Tanabe K, Yanagida M, Sakurai M, Amano M, Kaibuchi K, Inagaki M. Phosphorylation of vimentin by Rho-associated kinase at a unique amino-terminal site that is specifically phosphorylated during cytokinesis. J Biol Chem 1998, 273:11728–11738
68 Takemura M, Gomi H, Colucci-Guyon E, Itohara S. Protective role of phosphorylation in turnover of glial fibrillary acidic protein in mice. J Neurosci 2002, 22:6972–6979
69 Goto H, Yasui Y, Kawajiri A, Nigg EA, Terada Y, Tatsuka M, Nagata K, Inagaki M. Aurora-B phosphorylates the cleavage-furrow-specific vimentin phosphorylation in the cytokinetic process. J Biol Chem 2003, 278:8526–8530
70 Masters SC, Fu H. 14-3-3 proteins mediate an essential anti-apoptotic signal. J Biol Chem 2001, 276:45193–45200

DOI: 10.1093/brain/awh219 *Brain* (2004), **127**, 1917–1927

The regulatory role of natural killer cells in multiple sclerosis

Kazuya Takahashi,[1] Toshimasa Aranami,[1] Masumi Endoh,[1,2] Sachiko Miyake[1] and Takashi Yamamura[1]

[1]*Department of Immunology, National Institute of Neuroscience, National Center of Neurology and Psychiatry, 4-1-1 Ogawahigashi, Kodaira, Tokyo 187-8502 and* [2]*Department of Bioregulation, Leprosy Research Center, National Institute of Infectious Diseases, 4-2-1 Aoba, Higashimurayama, Tokyo 189-0002, Japan*

Correspondence to: Takashi Yamamura, Department of Immunology, National Institute of Neuroscience, National Center of Neurology and Psychiatry, 4-1-1 Ogawahigashi, Kodaira, Tokyo 187-8502, Japan
E-mail: yamamura@ncnp.go.jp

Summary

Multiple sclerosis is a chronic demyelinating disease of presumed autoimmune pathogenesis. The patients with multiple sclerosis typically shows alternating relapse and remission in the early stage of illness. We previously found that in the majority of multiple sclerosis patients in a state of remission, natural killer (NK) cells contain unusually high frequencies of the cells expressing CD95 (Fas) on their surface (>36.0%). Here we report that in such 'CD95$^+$ NK-high' patients, NK cells may actively suppress potentially pathogenic autoimmune T cells that can mediate the inflammatory responses in the CNS. Using peripheral blood mononuclear cells (PBMCs) derived from 'CD95$^+$ NK-high' or 'CD95$^+$ NK-low' multiple sclerosis in a state of remission, we studied the effect of NK cell depletion on the memory T cell response to myelin basic protein (MBP), a major target antigen of multiple sclerosis. When we stimulated PBMCs of the 'CD95$^+$ NK-high' multiple sclerosis after depleting CD56$^+$ NK cells, a significant proportion of CD4$^+$ T cells (1/2000 to 1/200) responded rapidly to MBP by secreting interferon (IFN)-γ, whereas such a rapid T cell response to MBP could not be detected in the presence of NK cells. Nor did we detect the memory response to MBP in the 'CD95$^+$ NK-low' multiple sclerosis patients in remission or healthy subjects, regardless of whether NK cells were depleted or not. Depletion of cells expressing CD16, another NK cell marker, also caused IFN-γ secretion from MBP-reactive CD4$^+$ T cells in the PBMCs from 'CD95$^+$ NK-high' multiple sclerosis. Moreover, we showed that NK cells from 'CD95$^+$ NK-high' multiple sclerosis could inhibit the antigen-driven secretion of IFN-γ by autologous MBP-specific T cell clones *in vitro*. These results indicate that NK cells may regulate activation of autoimmune memory T cells in an antigen non-specific fashion to maintain the clinical remission in 'CD95$^+$ NK-high' multiple sclerosis patients.

Keywords: multiple sclerosis; myelin basic protein; NK cell; NK2; T cell–NK cell interaction

Abbreviations: CBA = cytokine bead array; HLA = human leukocyte antigen; IFN = interferon; IL = interleukin; MBP = myelin basic protein; MS-rel = multiple sclerosis in relapse; MS-rem = multiple sclerosis in remission; NK = natural killer; NK2 = NK type 2; OVA = ovalbumin; PBMCs = peripheral blood mononuclear cells; PI = propidium iodide; PLP = proteolipid protein; TCC = T-cell clone; TNF = tumour necrosis factor

Received January 14, 2004. Revised March 18, 2004. Second revision April 10, 2004. Accepted April , 2004. Advanced Access publication June 30, 2004

Introduction

Multiple sclerosis is a chronic neurological disease the pathology of which is characterized by multiple foci of inflammatory demyelinating lesions accompanying a variable degree of axonal changes (Bjartmar and Trapp, 2001). Regarding the pathogenesis of multiple sclerosis, studies have indicated that autoimmune T cells targeting myelin components play a crucial role in mediating the inflammatory process, particularly in the early stages of relapsing–remitting multiple sclerosis (Steinman, 2001). A number of laboratories have studied the properties of potentially pathogenic autoimmune T cell clones (TCC) reactive to myelin antigens such as myelin basic protein (MBP) and proteolipid protein (PLP), which have been derived from the peripheral blood of multiple sclerosis (Ota *et al.*, 1990; Pette *et al.*, 1990; Martin *et al.*, 1991; Ohashi *et al.*, 1995). The large majority of the TCC are CD4$^+$ and produce T helper type 1 (Th1) cytokines

such as interferon (IFN)-γ after recognizing the myelin peptide bound to human leukocyte antigen (HLA)-DR molecules. These results are consistent with the idea that the inflammatory process of multiple sclerosis is triggered by invasion of autoimmune Th1 cells into the CNS, and that exogenous or endogenous factors altering the Th1/Th2 balance may influence the disease activity. The relevance of this postulate is actually supported by clinical observations that Th2-inducing medications, such as copolymer-1, are beneficial for multiple sclerosis (Duda *et al.*, 2000; Neuhaus *et al.*, 2000), and that administration of IFN-γ showed deleterious effects on multiple sclerosis in previous clinical trials (Panitch *et al.*, 1987).

Although there are a number of candidate target antigens for multiple sclerosis, MBP is thought to be a primary target for autoimmune T cells, at least in some patients (Bielekova *et al.*, 2000). It is of note that MBP- or PLP-specific TCC can be established not only from multiple sclerosis, but also from peripheral blood of healthy subjects, which raised the intriguing issue as to how healthy subjects are protected from self-attack by the potentially pathogenic autoimmune Th1 cells. Although much remains to be clarified, studies in the last decade have showed that regulatory cells are involved in prevention of or recovery from autoimmune diseases in rodent (Das *et al.*, 1997; Zhang *et al.*, 1997; Olivares-Villagomez *et al.*, 1998; Sakaguchi *et al.*, 2001). This allows us to speculate that regulatory cells may contribute to protecting healthy subjects from developing autoimmune diseases such as multiple sclerosis, or to prohibiting acute attacks or enhancing the recovery from clinical exacerbations in patients with relapsing–remitting multiple sclerosis.

Whereas regulatory cells constitute various lymphoid populations, substantial evidence supports that natural killer (NK) cells play significant roles in protecting against autoimmune diseases (Zhang *et al.*, 1997; Matsumoto *et al.*, 1998; Smeltz *et al.*, 1999). In fact, it has previously been demonstrated that NK cell depletion augments the severity of a model for multiple sclerosis, experimental autoimmune encephalomyelitis (EAE) (Zhang *et al.*, 1997; Matsumoto *et al.*, 1998), which can be induced by sensitization against CNS myelin component. Given that autoimmune Th1 cells would mediate the pathology of EAE, we propose a possible involvement of NK cells in suppressing autoimmune Th1 cells in multiple sclerosis.

With the hypothesis that NK cells may contribute to maintaining the remission in relapsing–remitting multiple sclerosis, we have previously examined the cytokine production and surface phenotype of NK cells freshly isolated from the peripheral blood mononuclear cells (PBMCs) of multiple sclerosis in remission (MS-rem) or relapse (MS-rel) (Takahashi *et al.*, 2001). The results demonstrate that NK cells in MS-rem (but not MS-rel) are characterized by a remarkable elevation of interleukin (IL)-5 mRNA and a decreased expression of IL-12Rβ2 mRNA, as well as a higher percentage of $CD95^+$ cells among the $CD56^+$ NK cells. These features of the cells are reminiscent of NK type 2 (NK2) cells, which can be induced *in vitro* in the presence of IL-4 and of anti-IL-12 antibodies (Peritt *et al.*, 1998). The NK2 cells induced from PBMCs of healthy subjects inhibit the generation of IFN-γ-secreting Th1 cells from the PBMCs of the same subjects (Takahashi *et al.*, 2001), leading us to postulate that NK2-like cells detected in MS-rem may play a regulatory role. While the NK2-like features were found to be lost in patients at acute relapsing state, they tended to be restored along with clinical recovery. Obviously, these results do not imply that clinically diagnosed MS-rem represents a homogeneous condition. In fact, the parameters characteristic for NK2-like cells (i.e. up-regulation of IL-5 mRNA and an increased frequency of $CD95^+$ cells) showed a substantial variance in MS-rem, indicating their heterogeneity.

More recently, we have noticed that MS-rem can be divided into two subgroups, '$CD95^+$ NK-high' and '$CD95^+$ NK-low', according to the frequency of $CD95^+$ cells among NK cells. Here, we demonstrate that these two groups significantly differ in the responsiveness to MBP *ex vivo* in an NK-cell-depleted condition. Namely, NK-deleted PBMCs from '$CD95^+$ NK-high' multiple sclerosis responded rapidly to MBP, as assessed by the frequency of IFN-γ-secreting $CD4^+$ T cells at 8 h after stimulation with MBP, whereas those from the '$CD95^+$ NK-low' or from healthy subjects responded only marginally. Moreover, we showed that NK cells from a '$CD95^+$ NK-high' multiple sclerosis could inhibit the antigen-driven secretion of IFN-γ by MBP-specific TCC established from the same patient. These results demonstrate, for the first time to our knowledge, that NK cell depletion leads to augmentation of memory T cell response to an autoantigen in human, and that an elaborate interplay between NK cells and MBP-specific memory T cells may be involved in the regulation of multiple sclerosis in '$CD95^+$ NK-high' patients.

Material and methods

Subjects

To clarify the heterogeneity among patients with MS-rem regarding NK cell phenotype, we first examined 30 patients with MS-rem (male/female = 11/19; aged 37.7 ± 11.1 years) for the lymphoid cell expression of CD95. As a control for multiple sclerosis, we examined 26 healthy sex- and age-matched subjects (male/female = 11/15; aged 39.9 ± 12.2 years). Furthermore, for a new cohort of 14 patients with MS-rem (male/female = four/10; aged 39.2 ± 10.7 years) (Table 1) and 14 healthy subjects (male/female = five/nine; aged 35.3 ± 8.0 years), we conducted the cytokine secretion assay as well as flow cytometer analysis for the frequency of $CD95^+$ NK cells. Two of the patients were examined again after a 1-year interval.

Written informed consent was obtained from all patients and healthy volunteers and the study was approved by the Ethics Committee of the National Center of Neuroscience (NCNP). All patients fulfilled standard criteria for the diagnosis of relapsing–remitting multiple sclerosis (Poser *et al.*, 1983; McDonald *et al.*, 2001). The clinical status of multiple sclerosis (MS-rem or MS-rel) was operationally determined as described previously (Takahashi *et al.*, 2001). In brief, we selected MS-rem patients for study who had been clinically stable without any immunosuppressive medications for >3 months, and had shown no sign of new lesions as assessed by a recent MRI scan with gadolinium enhancement. None of our patients represented the pure optic-spinal form of multiple sclerosis (Misu *et al.*, 2002), which may be rather unique to Japanese populations.

Table 1 *List of the PBMC samples examined for the frequency of memory Th1 cells*

Information on patients			
PBMC code	Age (years)/sex	CD95$^+$ NK frequency	EDSS#
#1	43/M	High	2.5
#2	30/F	High	2.5
#3	53/M	High	1.0
#4	39/F	High	3.5
#5	28/F	High	1.0
#6*	35/M	Low	2.0
#7**	57/F	Low	3.0
#8	31/M	Low	1.0
#9	29/F	Low	3.0
#10	38/F	Low	2.0
#11	59/F	High	3.5
#12*	36/M	High	2.0
#13**	58/F	High	3.0
#14	33/F	High	6.5
#15	29/F	Low	1.0
#16	45/F	Low	4.0

The samples marked with * or ** are derived from the same patients, with an interval of 1 year between samples. The phenotype of both of these patients changed from 'CD95$^+$ NK-low' to 'CD95$^+$ NK-high'. M = male; F = female; EDSS = Expanded Disability Status Scale.

Reagents

Anti-CD3-FITC or -ECD, anti-CD4-PC5, anti-CD8-FITC, anti-CD16-Phytoerythrin, and anti-CD56-PC5 or -PE mAbs were purchased from IMMUNOTECH (Marseille, France). Anti-CD57-FITC, anti-CD69-PE, anti-CD94-FITC, anti-CD95-FITC, -Cych or -PE, anti-CD158a-FITC, anti-NKB1-FITC, and anti-HLA-DR-FITC mAbs were purchased from BD PharMingen (San Jose, CA, USA). Human MBP was purified with a modification of previously described methods (Deibler *et al.*, 1972, 1995).

Cell preparation and NK cell deletion

Shortly after drawing peripheral blood, PBMCs were separated by density gradient centrifugation with Ficoll-Hypaque™ PLUS (Amersham Biosciences, Uppsala, Sweden). They were washed three times in phosphate-buffered saline (PBS), and resuspended at 1 $\times$ 10^6 cells/ml in AIM-V culture medium (Invitrogen Corp., Carlsbad, CA, USA) containing 2 mM L-glutamine, 100 U/ml penicillin and 100 µg/ml streptomycin (Life Technologies, Rockville, MD, USA). NK cells were depleted from the PBMCs with either CD56- or CD16-MicroBeads (Miltenyi Biotech, Gradbach, Germany), following the protocol provided by the manufacturer.

T cell clones

CD4$^+$ TCC were generated from a 'CD95$^+$ NK-high' multiple sclerosis patient (HLA-DRB1*1502) by repeated selection against human whole MBP with modification of a previously described method (Pette *et al.*, 1990). The TCC proliferated and secreted Th1 cytokines specifically in response to MBP, and the proliferative response and cytokine production was greatly reduced in the presence of antibodies against HLA-DR. The DR-restricted clone cells were grown in AIM-V medium supplemented with 2 mM L-glutamine, 100 U/ml penicillin and 100 µg/ml streptomycin.

T-cell stimulation with MBP

To assess the presence of memory MBP-reactive T cells in the peripheral blood, fresh PBMCs or NK-deleted PBMCs were stimulated for 8 h with 10 µg/ml MBP in 96-well round-bottomed plates at 2×10^5 cells/well, and then analysed for the presence of IFN-γ-secreting cells using the cytokine secretion assay. To evaluate the regulatory function of NK cells from 'CD95$^+$ NK-high' multiple sclerosis, resting cells of MBP-specific TCC (2×10^4 cells/well) were stimulated with 10 µg/ml MBP in the presence of X-irradiated (5000 rad) autologous total PBMCs or CD56$^+$ NK-deleted PBMCs (1×10^5 cells/well) for 8 h prior to the cytokine secretion assay, and for 60 h to determine the proliferation of the TCC. To assess cell proliferation, we counted incorporation of [^{3}H]thymidine (1 µCi/well) during the final 12 h with a beta-1205 counter (Pharmacia, Uppsala, Sweden).

Cytokine secretion assay

We used a commercial kit from Miltenyi Biotech to identify T cells secreting IFN-γ. The principle of this assay has been described previously (Manz *et al.*, 1995). Briefly, cells were stained with IFN-γ capture antibody 8 h after stimulation with MBP or ovalbumin (OVA), then washed and cultured again for 45 min. They were stained with PE-conjugated IFN-γ detection antibody, together with anti-human CD3-FITC and -CD4-PC5, then washed and resuspended in PBS containing propidium iodide (PI) (BD PharMingen). Samples were analysed using flow cytometry.

Cytokine bead array

The levels of IL-2, -4, -5, -10, tumour necrosis factor (TNF)-α and IFN-γ in the culture supernatants were measured by cytokine bead array (CBA) (BD PharMingen), in which six bead populations with distinct fluorescence intensities are coated with capture antibodies specific for each cytokine (Cook *et al.*, 2001). The cytokine capture beads were mixed with the PE-conjugated detection antibodies and then incubated with recombinant standards or supernatant samples to form sandwich complexes. After washing the beads, sample data were acquired using the flow cytometer and were analysed with the BD CBA Analysis Software® (BD PharMingen).

Results

An increased frequency of CD95$^+$ NK cells distinguishes a subgroup of multiple sclerosis

As we have reported previously (Takahashi *et al.*, 2001), whereas proportions of CD3$^-$ CD56$^+$ NK cells in fresh PBMCs weakly express CD95 on their surface, the frequency of CD95$^+$ NK cells is significantly elevated in MS-rem as compared with healthy subjects or MS-rel. We have further noticed that MS-rem can be divided into two subgroups according to the frequency (%) of CD95$^+$ cells among NK cells (Fig. 1A; see also the left panels in Figs 1B and 2A, showing the distinction between CD95$^+$ and CD95$^-$ cells). When we determined the mean +2 SD value for healthy subjects (35.86%) as an upper boundary for healthy subjects,

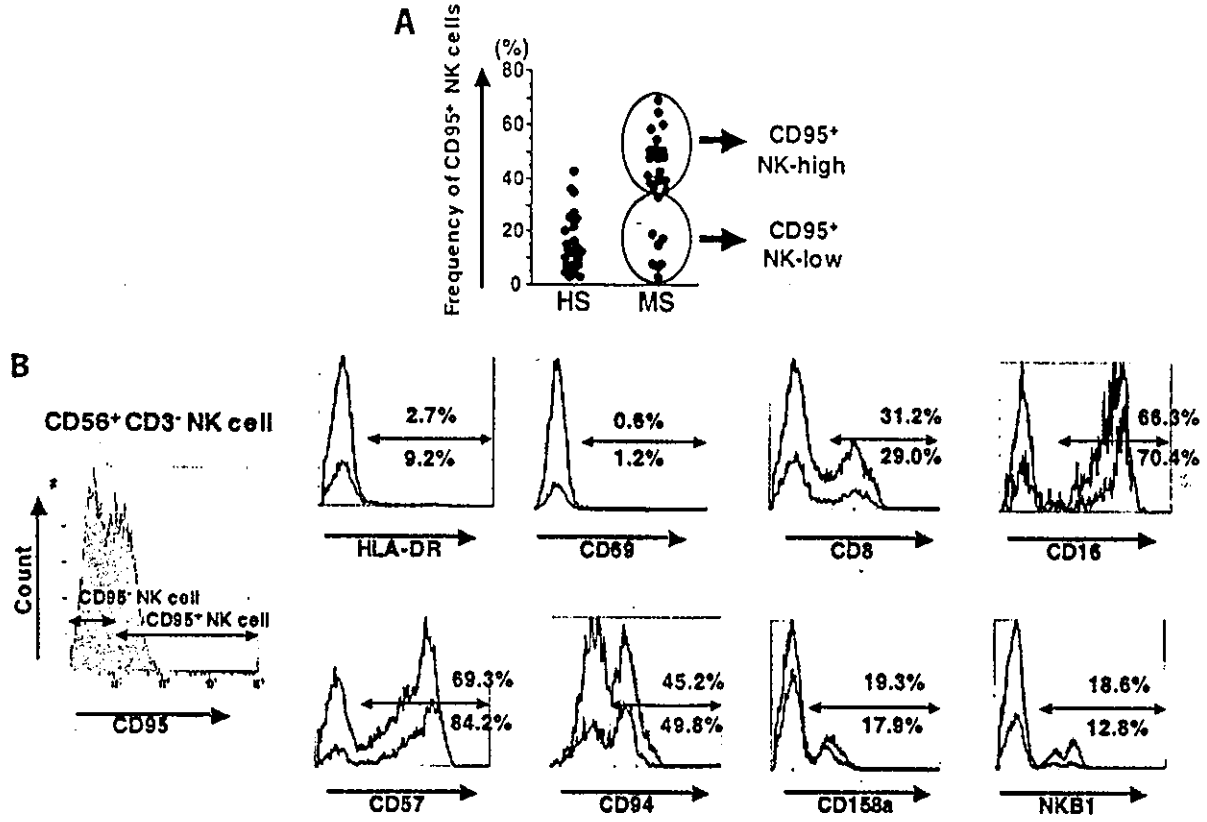

Fig. 1 Characterization of CD95$^+$ NK cells from 'CD95$^+$ NK-high' multiple sclerosis. (**A**) Multiple sclerosis patients in remission (MS-rem) can be subgrouped into 'CD95$^+$ NK-high' and 'CD95$^+$ NK-low'. Freshly isolated PBMCs from 26 healthy subjects or 30 MS-rem were stained with the combination of anti-CD3-FITC, -CD56-PC5 and -CD95-PE, and evaluated for the frequency of CD95$^+$ cells in the CD56$^+$CD3$^-$ NK cell population (the fluorescence intensity for CD95 expression is shown in the histograms in B and Fig. 2A). Note that flow fluorocytometric analysis was completed within 2 h after drawing blood in order to avoid spontaneous death of CD95$^+$ cells. (**B**) Comparison of CD95$^+$ versus CD95$^-$ NK cells in the expression of various surface molecules. We stained the PBMCs from 'CD95$^+$ NK-high' patients with the panel of antibodies for surface molecules expressed by NK cells. Red lines represent the histogram gated for CD95$^-$ NK cells and blue lines for CD95$^+$ NK cells. Values in red and in blue represent the positive percentage in CD95$^-$ and CD95$^+$ cells, respectively. As indicated, CD95$^+$ NK cells did not differ significantly from CD95$^-$ NK cells in the staining pattern for each antibody regarding the proportion of positive cells as well as the mean fluorescence intensity. Shown are the results of a representative case.

three-quarters of MS-rem had a percentage value higher than this boundary. We defined these patients in remission with a higher frequency of CD95$^+$ cells in NK cells as 'CD95$^+$ NK-high' multiple sclerosis, and the rest as 'CD95$^+$ NK-low' (Fig. 1A). In contrast to CD56$^+$ NK cells, CD3$^+$CD56$^-$ T cells and CD3$^+$CD56$^+$ NK T cells were not different between healthy subjects and multiple sclerosis patients as regards the frequency of CD95$^+$ cells (data not shown), which directed our attention to the analysis of CD56$^+$ NK cells.

Because NK cells from MS-rem were found to express a larger amount IL-5 mRNA, and since they were neither defective in cytolytic function nor reduced in number (Takahashi *et al.*, 2001), we hypothesized that the CD95 expression may reflect an activation state of the NK cells. To test this hypothesis, we compared the CD95$^+$ and CD95$^-$ NK populations derived from 'CD95$^+$ NK-high' patients by flow cytometry. Histogram plot analysis for the proportion of positive cells and for mean fluorescence intensity showed that the two populations are analogous in the expression of HLA-DR, CD69, CD8, CD16, CD57, CD94, CD158a and NKB1 (Fig. 1B). Whereas HLA-DR and CD69 molecules are regarded as cell activation markers, few populations of CD95$^+$ NK cells from multiple sclerosis or healthy subjects expressed these molecules. These results do not support the idea that the CD95$^+$ NK cells are in a state of activation, nor do they indicate that the CD95$^+$ cells represent a unique subset of monoclonal or oligoclonal origin. It has recently been suggested that CD56^{bright} NK cells may represent a distinct subset (Jacobs *et al.*, 2001). However, we saw no difference in the proportion of CD56^{bright} cells between CD95$^+$ and CD95$^-$ NK cells (data not shown).

CD56$^+$ NK cell depletion induces the rapid activation of MBP-reactive memory T cells in PBMCs from 'CD95$^+$ NK-high' multiple sclerosis

We have previously shown that the CD95$^+$ NK cells found in multiple sclerosis patients resemble the NK cells that can be induced in culture in the presence of IL-4 and anti-IL-12

mAb [referred to as 'NK2-like cells' according to the definition by Peritt *et al.* (1998)]. We also found that Peritt's NK2 cells induced *in vitro* inhibited the induction of IFN-γ-secreting T cells from peripheral T cells after stimulation with phorbol myristate acetate and ionomycin (Takahashi *et al.*, 2001). Based on these observations, we speculated that NK cells might prohibit Th1 cell activation in the remission of multiple sclerosis in an antigen-non-specific manner, and contribute to maintaining the remission. However, it remained an open question as to whether the NK2-like cells found in MS-rem would indeed regulate pathogenic autoimmune T cells *in vivo*. To investigate functions of NK cells in MS-rem, we evaluated the effect of NK cell depletion on the peripheral T cell response to MBP, a major target antigen of multiple sclerosis (Bielekova *et al.*, 2000). In brief, we depleted $CD56^+$ cells from the PBMCs with a magnetic sorter, and then stimulated the NK-deleted populations as well as whole PBMCs with MBP *in vitro* for 8–24 h. Subsequently, we detected the antigen-responsive T cells based on the secretion of IFN-γ (Manz *et al.*, 1995). The preparatory experiments revealed that 8 h of stimulation provides an optimal condition yielding a low background (0–0.03%). This novel assay enables us to selectively detect memory-type Th1 cells that can respond rapidly to antigen, whereas previous assays that depend on long-term cultures (Pette *et al.*, 1990; Martin *et al.*, 1992) evaluate not only memory but also naive T cells. Of note, there is a general consensus that peripheral blood of multiple sclerosis patients contains MBP-reactive T cells that are activated and/or differentiated into memory T cells (Allegretta *et al.*, 1990; Martin *et al.*, 1992; Zhang *et al.*, 1994; Lovett-Racke *et al.*, 1998; Scholz *et al.*, 1998).

We examined 16 PBMC samples from 14 MS-rem patients (nine samples from '$CD95^+$ NK-high', and seven from '$CD95^+$ NK-low') and 14 healthy subjects (see Table 1). When freshly isolated PBMCs were stimulated with MBP before NK cell depletion, four MS-rem and five healthy subjects samples showed a marginal response to MBP (0.01–0.03% increase of IFN-γ-positive cells among $CD4^+$ T cells). We did not find any significant response to MBP with the other PBMC samples. In contrast, when cells were stimulated with MBP after deleting $CD56^+$ NK cells, a significant response with a stimulatory index >3 was detected in seven of the nine '$CD95^+$ NK-high' samples, and a marginal response was detected in two (Fig. 2A and B). Of note, none of the NK-deleted samples from the '$CD95^+$ NK-low' patients and healthy subjects showed a definitive response to MBP. The difference for the '$CD95^+$ NK-high' versus the '$CD95^+$ NK-low' or healthy subjects was statistically significant (Fig. 2B). These *ex vivo* experiments have revealed that the '$CD95^+$ NK-high' patients may possess a higher number of T cells that can rapidly respond to MBP (MBP-specific memory T cells), compared with '$CD95^+$ NK-low' MS-rem or healthy subjects. In other words, they provide strong evidence for clonal expansion of memory autopathogenic T cells in the '$CD95^+$ NK-high' patients. However, as we could demonstrate an increase of the memory autoimmune T cells only after depleting NK cells, we interpreted that the potentially hazardous autoimmune T cells are being controlled by counter-regulatory NK cells in the '$CD95^+$ NK-high' patients. Of note, previous studies relying on alternative assays have revealed the presence of MBP-reactive T cells with activated and/or memory phenotypes at similar high frequencies in not all, but a major portion, of multiple sclerosis patients (Allegretta *et al.*, 1990; Zhang *et al.*, 1994; Bieganowska *et al.*, 1997; Lovett-Racke *et al.*, 1998; Scholz *et al.*, 1998; Illés *et al.*, 1999).

We conducted the same assay with a foreign antigen OVA in three of the '$CD95^+$ NK-high' (PBMC codes #3, #4 and #5 in Table 1) and one of the '$CD95^+$ NK-low' samples (#6). However, OVA-reactive T cells could not be detected in any sample of the fresh or NK-deleted PBMCs (data not shown). Because NK cells cannot discriminate T cells with different antigen specificities, the negative response to OVA in the four multiple sclerosis patients was interpreted to mean that they do not possess clonally expanded memory T cells reactive to OVA.

Depletion of $CD16^+$ NK cells also allows detection of MBP-reactive memory T cells in PBMCs from '$CD95^+$ NK-high' multiple sclerosis

Although we used anti-CD56 magnetic beads to deplete NK cells in the above experiments, the method would also deplete $CD3^+CD56^+$ NK T cells that may possibly play a role in the regulation of autoimmunity. To evaluate the possible contribution of $CD3^+CD56^+$ NK T cells, we next depleted NK cells from PBMCs from two '$CD95^+$ NK-high' patients on the basis of their expression of CD16. We found that after treatment with CD16-MicroBeads, almost all of $CD56^+$ NK cells are deleted, but $CD56^+CD3^+$ NKT cells remain largely untouched (Fig. 3A). However, like $CD56^+$-cell-deleted PBMCs, the $CD16^+$-cell-deleted PBMCs responded to MBP, as assessed by the induction of IFN-γ-secreting $CD4^+$ T cells (Fig. 3B). The responses found in the two patients were considered significant with regard to both percentage increase of IFN-γ-secreting cells (0.08% and 0.04%) and the stimulatory index (9.0 and 5.0) obtained after MBP stimulation. This result indicates that responsible cells to regulate autoimmune T cells in '$CD95^+$ NK-high' multiple sclerosis are not $CD56^+CD3^+$ NK T cells but NK cells.

Unfortunately, it remains unclear whether only $CD95^+$ NK cells play a regulatory role in '$CD95^+$ NK-high' multiple sclerosis or whether $CD95^-$ cells could also exhibit regulatory functions in the patients. We attempted to compare directly the function of $CD95^+$ and $CD95^-$ populations. However, isolation of $CD95^+$ NK cells with a cell sorter invariably induced cell activation as revealed by the expression of various activation markers. Furthermore, the isolated cells tended to die rapidly, probably due to CD95 ligation by the antibody (data not shown).

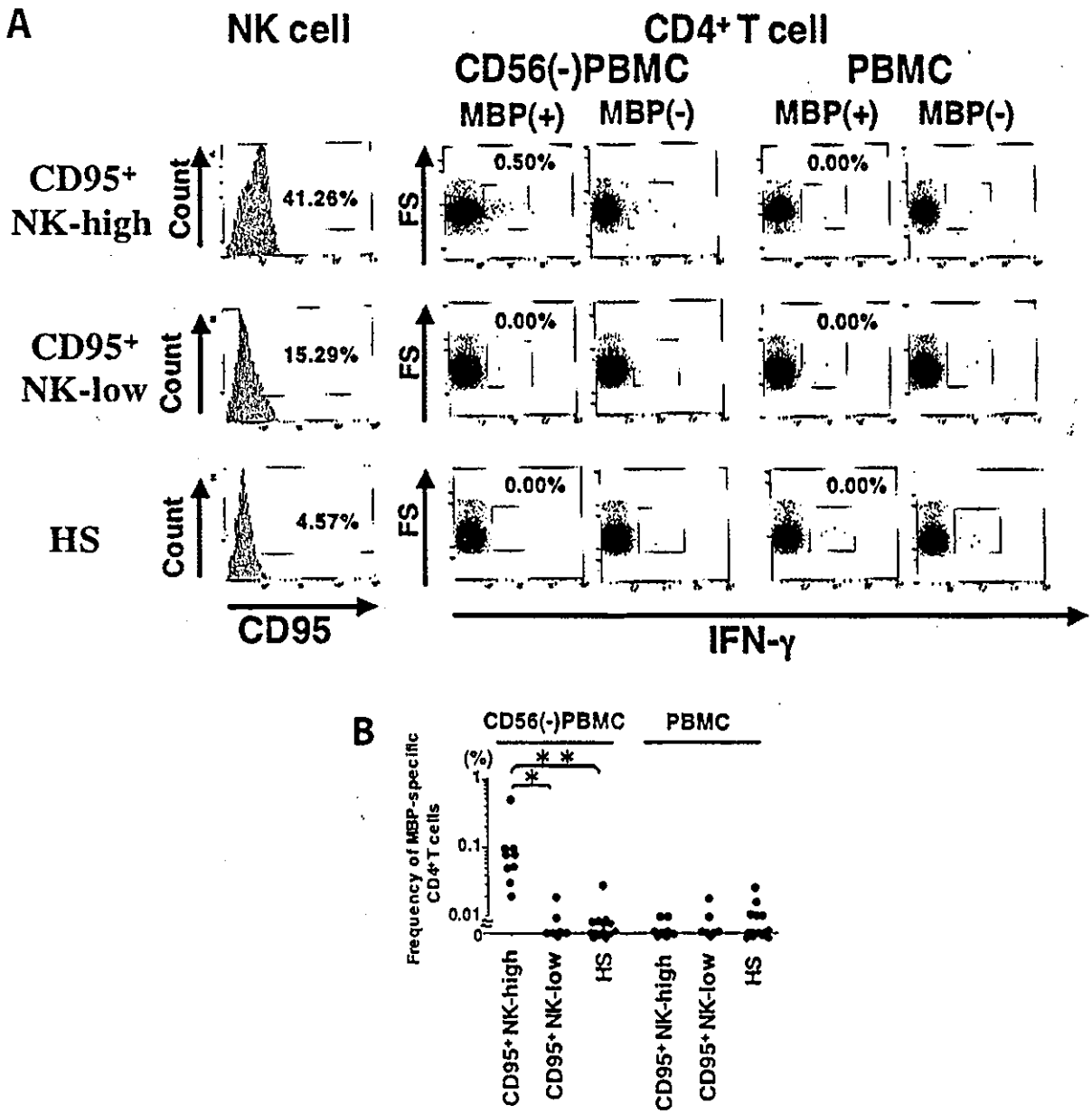

Fig. 2 Evidence for the role of NK cells in the regulation of MBP-reactive memory T cells in 'CD95$^+$ NK-high' multiple sclerosis. (A) IFN-γ secretion assay for NK-cell-deleted PBMCs and freshly isolated PBMCs. Whole PBMCs or PBMCs depleted for CD56$^+$ NK cells [CD56(−) PBMC] from the 'CD95$^+$ NK-high' multiple sclerosis (n = 9), 'CD95$^+$ NK-low' multiple sclerosis (n = 7) or healthy subjects (n = 14) were stimulated with 10 μg/ml of human MBP for 8 h for the IFN-γ secretion assay. The cells were also stained with anti-CD4-PC5 and -CD3-FITC, and the CD4$^+$CD3$^+$ and PI$^-$ cells were gated for analysis. Here we show representative results from 'CD95$^+$ NK-high' (*top*), 'CD95$^+$ NK-low' (*middle*) and healthy subjects (*bottom*). The IFN-γ-secreting CD4$^+$ T cells are shown as red dots; blue dots represent IFN-γ-négative cells. The histograms demonstrate the level of CD95 expression on the fresh CD56$^+$ NK cells from each individual, and the attached values show the frequency of CD95$^+$ cells. (B) Frequency (%) of MBP-reactive memory T cells among CD4$^+$ T cells. By using the cytokine secretion assay, we determined the frequency of IFN-γ-positive cells among CD4$^+$ T cells in each individual after culture with or without MBP. Here we plot the Δ% values [(%) with MBP − (%) without MBP], which represent the frequency of MBP-reactive CD4$^+$ T cells in each subject. Kruskal–Wallis test with Scheffe's F *post hoc* test was used for statistical analysis. *P < 0.05; **P < 0.02.

NK cells from 'CD95$^+$ NK-high' multiple sclerosis inhibit IFN-γ production by MBP-reactive T cell clones

To analyse how the NK cells from 'CD95$^+$ NK-high' multiple sclerosis efficiently control autoimmune T cell responses, we established three MBP-specific TCC from a 'CD95$^+$ NK-high' patient. These TCC proliferated and secreted IFN-γ, TNF-α, IL-2 and IL-5 in response to MBP presented by irradiated, fresh autologous PBMCs. Using the proliferation response and cytokine secretion by